

## Lehigh University Lehigh Preserve

---

Fritz Laboratory Reports

Civil and Environmental Engineering

---

1966

# Inelastic lateral-torsional buckling of beam-columns, Proc. ASCE, Vol. 92, ST 2, April 1966, Publication No. 299

T. V. Galambos

Y. Fukumoto

Follow this and additional works at: <http://preserve.lehigh.edu/engr-civil-environmental-fritz-lab-reports>

---

### Recommended Citation

Galambos, T. V. and Fukumoto, Y., "Inelastic lateral-torsional buckling of beam-columns, Proc. ASCE, Vol. 92, ST 2, April 1966, Publication No. 299" (1966). *Fritz Laboratory Reports*. Paper 1345.  
<http://preserve.lehigh.edu/engr-civil-environmental-fritz-lab-reports/1345>

This Technical Report is brought to you for free and open access by the Civil and Environmental Engineering at Lehigh Preserve. It has been accepted for inclusion in Fritz Laboratory Reports by an authorized administrator of Lehigh Preserve. For more information, please contact [preserve@lehigh.edu](mailto:preserve@lehigh.edu).

Welded Continuous Frames and Their Components

INELASTIC LATERAL-TORSIONAL BUCKLING  
OF BEAM-COLUMNS

by

Theodore V. Galambos

and

Yuhshi Fukumoto

This work has been carried out as part of an investigation sponsored jointly by the Welding Research Council and the Department of the Navy with funds furnished by the following:

American Institute of Steel Construction  
American Iron and Steel Institute  
Institute of Research, Lehigh University  
Column Research Council (advisory)  
Office of Naval Research (Contract No. 610 (03) )  
Bureau of Ships  
Bureau of Yards and Docks

Reproduction of this report in whole or in part is permitted for any purpose of the United States Government.

Fritz Engineering Laboratory  
Lehigh University  
Bethlehem, Pennsylvania

August 1963

Fritz Engineering Laboratory Report No. 205A.34

SYNOPSIS

In this report a method is presented for the determination of the inelastic lateral-torsional buckling strength of as-rolled steel wide-flange beam-columns. The beam-columns are subjected to an axial force and to bending moments applied at one end only. The end-moments cause bending about the strong axis of the members, and the effects of initial residual stresses are included in the analysis.

The solutions are obtained on the basis of a finite difference approximation of the differential equations with variable coefficients, the resulting characteristic determinant being solved numerically by a digital computer.

TABLE OF CONTENTS

	SYNOPSIS	i
I	INTRODUCTION	1
II	THE DIFFERENTIAL EQUATIONS OF LATERAL-TORSIONAL BUCKLING	4
III	DETERMINATION OF THE STIFFNESS PARAMETERS	11
IV	LATERAL-TORSIONAL BUCKLING STRENGTH	24
V	SUMMARY	34
VI	ACKNOWLEDGEMENTS	37
VII	NOTATIONS	38
VIII	TABLES AND FIGURES	42
IX	REFERENCES	

## I. INTRODUCTION

A perfectly straight wide-flange member which is subjected to an axial force and to end moments about the strong axis of the section will deflect in the plane of the applied moments as long as the moments and the axial force are below certain critical values. At the instant of the attainment of the critical loading, bifurcation of the equilibrium will take place and failure is initiated by lateral deflection and twisting of the member. (1) (2)

Typical beam-column behavior is illustrated in Fig. 1, where the schematic relationship between the applied end moment  $M_0$  and the resulting end slope  $\theta$  is illustrated for a wide-flange member bent about its x-axis. The axial force  $P$  is assumed to remain constant as  $M_0$  is increased from zero to its final value.

The  $M_0$ - $\theta$  relationship is seen to have two branch curves: (1) The upper branch results if no lateral-torsional buckling is assumed to occur. In this case failure will be due to excessive bending in the plane of the applied moments, with no deformations at all except in this plane. (3) This

curve represents the optimum performance of the member.

(2) If the lateral bracing is insufficient, lateral-torsional buckling will set in at  $M_o = M_{oCR}$  and failure will occur at a moment  $M_{o1MAX}$  which is lower than the ultimate strength  $M_{o2MAX}$ .

Attainment of the maximum moment is always accompanied by yielding of part of the member. Whereas methods are available to determine the value of the maximum moment  $M_{o2MAX}$  if failure is by excessive deflection in the plane of loading, (3) no such methods are presently available to compute  $M_{o1MAX}$ . Experiments on steel wide-flange beam-columns have shown however, that the increase of the moment capacity above  $M_{oCR}$  (the moment at the start of lateral-torsional buckling) is only slight, and therefore this moment can be considered to be a good index of the beam-column strength when failure is due to lateral-torsional buckling. (4) (5)

The work in this report is concerned with the determination of the critical moment when the inception of lateral-torsional buckling occurs after the member has already partially yielded. The method of determining the critical

moment is illustrated by considering a beam-column which is loaded by one end moment only (see sketch in Fig. 1).

The problem of elastic lateral-torsional buckling has been thoroughly investigated. (1)(2)(6) For buckling in the inelastic range the reduction of the stiffeners governing the buckling behavior must be considered. Solutions have been presented for beams (7)(8)(9)(10)(11)(12)(13) and beam-columns (14) under moments producing symmetric deformations. This report considers the influence of non-uniform bending. (15)

## II. THE DIFFERENTIAL EQUATIONS OF LATERAL-TORSIONAL BUCKLING

### Assumptions

The differential equations of lateral-torsional buckling derived herein are based on the following specific conditions and assumptions:

- (1) The axial thrust  $P$  acts through the original centroidal axis of the member and it retains its direction even after buckling has taken place.
- (2) The moments  $M_0$  are applied at the ends of the member only, such that they cause bending about the major axis of the cross section. No transverse loads are applied between supports.
- (3) The beam-columns are as-rolled steel wide-flange shapes which are initially free of crookedness and for which the cross-sectional dimensions do not vary with the length.
- (4) The ends of the members are simply supported with respect to lateral-torsional buckling. The



boundary conditions are therefore

$$u = u'' = \beta = \beta'' = 0 \text{ at } z = 0 \text{ and } z = L.$$

- (5) The stress-strain diagram of the material is ideally elastic-plastic. (Fig. 2)
- (6) The residual stress pattern is symmetric and the residual stresses are distributed in the flanges and in the web as shown in Fig. 3. (16)

Equilibrium requires that

$$\sigma_{rt} = \sigma_{rc} \left[ \frac{bt}{bt + w(d-2t)} \right] \quad (1)$$

where  $b$ ,  $t$ ,  $d$ , and  $w$  are the dimensions of the cross section,  $\sigma_{rt}$  is the maximum tensile residual stress and  $\sigma_{rc}$  is the maximum compressive residual stress.

- (7) The cross section retains its original shape and no local buckling is assumed to occur before bifurcation.
- (8) The deflections are small in comparison with the cross sectional dimensions of the member.

### Equations of Equilibrium

Equilibrium equations will be formulated in the following derivation for a deformed cross section located at a distance  $z$  from the end of the member (Fig. 4). The axial thrust  $P$  is applied with eccentricities  $e_{yB}$  at  $z = 0$  and  $e_{yT}$  at  $z = L$ , where  $e_{yB}$  and  $e_{yT}$  are in the  $zy$  plane, which is also the plane of symmetry of the cross section. The deformed location of the cross section at  $z$  is fully defined by the displacements  $u$  and  $v$  of the shear center  $S$ , and by the twisting angle  $\beta$  (Fig. 4). As will be explained later, the shear center  $S$  does not coincide with the centroid of the cross section after yielding, and therefore this fact must be considered in the formulation of the equilibrium conditions. Because of the symmetry of the residual stresses about the  $y$ -axis, (Fig. 3),  $S$  will remain on this axis (Fig. 4).

If the direction of the moments is positive as indicated in Fig. 5, the bending moments in the  $x$  and  $y$  directions at any point  $z$  are equal to

$$M_x = P \left\{ \left[ \rho + (1 - \rho)z/L \right] e_{yT} - v \right\} \quad (2)$$

$$M_y = P (u + \beta y_0) \quad (3)$$

where  $\rho = \frac{e_{yB}}{e_{yT}}$  and the end  $z = 0$  is chosen such that  $e_{yB} \leq e_{yT}$ .

In addition to the coordinates  $x$ ,  $y$ , and  $z$ , there are coordinates  $\xi$ ,  $\eta$ , and  $\zeta$  associated with the deformed cross-section. The axes  $\xi$  and  $\eta$  are shown in Fig. 4, and the axis  $\zeta$  is in the direction of the tangent to the center line of the member. The relationships for the direction cosines between the two axis systems are: (2)

	$\xi$	$\eta$	$\zeta$
$x$	1	$-\beta$	$\frac{du}{dz}$
$y$	$\beta$	1	$\frac{dv}{dz}$
$z$	$-\frac{du}{dz}$	$-\frac{dv}{dz}$	1

The components of  $M_x$  and  $M_y$  in the  $\xi$ ,  $\eta$  and  $\zeta$  directions are obtained from the table of directions cosines; that is,

$$M_\xi = M_x + \beta M_y \quad (4)$$

$$M_\eta = -\beta M_x + M_y \quad (5)$$

$$M_{\zeta'} = -M_x \frac{du}{dz} - M_y \frac{dv}{dz} \quad (6)$$

The positive directions of these moments are as shown in Fig. 6. In addition to the torque  $M_{\zeta'}$ , there are three other components of the twisting moment:

$$M_{\zeta 2} = P y_0 \frac{du}{dz} \quad (7)$$

$$M_{\zeta 3} = \int_A \sigma s^2 \frac{d\beta}{dz} dA \quad (8)$$

$$M_{\zeta 4} = P \left[ \frac{e_{\gamma T} (1 - \rho) U}{L} \right] \quad (9)$$

The torque  $M_{\zeta 2}$  is due to the component of  $P$  causing twisting about the shear center  $S'$  (Fig. 7),  $M_{\zeta 3}$  is caused by the components of the normal stresses on the warped cross section, and  $M_{\zeta 4}$  is the twist of the end reactions (see Fig. 8) about the shear center.

The total torsional moment  $M_{\zeta}$  is thus equal to

$$\begin{aligned} M_{\zeta} &= M_{\zeta 1} + M_{\zeta 2} + M_{\zeta 3} + M_{\zeta 4} \\ &= (Py_0 - M_x) \frac{du}{dz} - M_y \frac{dv}{dz} + \int_A \sigma s^2 dA \frac{d\beta}{dz} + \left[ P \frac{e_{yT}(1-\rho)}{L} \right] u \end{aligned} \quad (10)$$

Substituting  $M_x$  and  $M_y$  of Eqs. (2) and (3) into Eqs. (4), (5) and (10),  $M_{\zeta}$ ,  $M_2$ , and  $M_{\zeta}$  will be equal to the following expressions if small quantities of higher order are neglected:

$$M_{\zeta} = P \left\{ \left[ \rho + (1-\rho) \frac{z}{L} \right] e_{yT} - v \right\} \quad (11)$$

$$M_2 = -P \left\{ \left[ \rho + (1-\rho) \frac{z}{L} \right] e_{yT} \right\} \beta + P(u + \beta y_0) \quad (12)$$

$$M_{\zeta} = P \left\{ y_0 - \left[ \rho + (1-\rho) \frac{z}{L} \right] e_{yT} \right\} \frac{du}{dz} + \int_A \sigma s^2 dA \frac{d\beta}{dz} + P \left[ \frac{e_{yT}(1-\rho)}{L} \right] u \quad (13)$$

The differential equations of equilibrium are obtained by setting the external moments equal to the internal moments (2)

$$M_{\zeta} = B_x \frac{d^2 v}{dz^2} \quad (14)$$

$$M_2 = -B_y \frac{d^2 u}{dz^2} \quad (15)$$

$$M_{\zeta} = C_T \frac{d\beta}{dz} - C_w \frac{d^3 \beta}{dz^3} \quad (16)$$

In Eqs. (14), (15), and (16), the terms  $B_x$  and  $B_y$  signify the principal flexural rigidities of the cross section,  $C_T$  is the St. Venant torsional stiffness, and  $C_w$  is the warping stiffness. Combining Eqs. (11), (12), and (13) with Eqs. (14), (15), and (16), the following differential equations are obtained:

$$B_x \frac{d^2 v}{dz^2} + P \left\{ v - \left[ \rho + (1-\rho) \frac{z}{L} \right] e_{yT} \right\} = 0 \quad (17)$$

$$B_y \frac{d^2 u}{dz^2} + P(u + \rho y_0) - P \left\{ \left[ \rho + (1-\rho) \frac{z}{L} \right] e_{yT} \right\} \rho = 0 \quad (18)$$

$$C_w \frac{d^3 \beta}{dz^3} - \left( C_T - \int_A \sigma_s^2 dA \right) \frac{d\beta}{dz} + P \left\{ y_0 - \left[ \rho + (1-\rho) \frac{z}{L} \right] e_{yT} \right\} \frac{du}{dz} + P \left[ \frac{e_{yT}(1-\rho)}{L} \right] u = 0 \quad (19)$$

Since Eq. (17) does not involve the lateral deflection  $u$  and the twist  $\beta$ , it pertains to an unbuckled deflection configuration and is of no further interest here.

Further discussion in this paper will be limited to the case where  $e_{yB} = 0$  (that is only one end moment). The two differential equations governing lateral-torsional buckling are then (from Eqs. (18) and (19) with  $\rho = 0$ ) equal to:

$$B_y \frac{d^2 u}{dz^2} + P u - \left( M_0 \frac{z}{L} - P y_0 \right) \beta = 0 \quad (20)$$

$$C_w \frac{d^3 \beta}{dz^3} - \left( C_T - \int_A \sigma_s^2 dA \right) \frac{d\beta}{dz} - \left( M_0 \frac{z}{L} - P y_0 \right) \frac{du}{dz} + \frac{M_0}{L} u = 0 \quad (21)$$

These equations cannot be solved directly because of the non-uniform moment term  $\frac{M_0 z}{L}$ , and because the coefficients of the deformations  $u$  and  $\beta$  vary with the different patterns of yielding due to the variation of the moment along the length of the member. A numerical solution based on finite difference equations at each pivotal point by first order central differences with the spacing  $h = L/n$  (where  $n$  is the number of subdivisions along the length of the member) results in the following equations:

$$u_{i-1} - \left(2 - \frac{Ph^2}{B_y}\right) u_i + u_{i+1} - \left(\frac{M_0 z}{L} - Py_0\right) \frac{h^2}{B_y} \beta_i = 0 \quad (22)$$

$$\begin{aligned} & \left(\frac{M_0 z}{L} - Py_0\right) \frac{h^2}{C_T} u_{i-1} + \frac{M_0 z h^3}{L C_T} u_i - \left(\frac{M_0 z}{L} - Py_0\right) \frac{h^2}{C_T} u_{i+1} \\ & - \frac{C_w}{C_T} \beta_{i-2} + \left[2 \frac{C_w}{C_T} - \left(1 - \frac{\int \sigma_x^2 dA}{C_T}\right) h^2\right] \beta_{i-1} + [0] \beta_i \\ & - \left[2 \frac{C_w}{C_T} - \left(1 - \frac{\int \sigma_x^2 dA}{C_T}\right) h^2\right] \beta_{i+1} + \frac{C_w}{C_T} \beta_{i+2} = 0 \end{aligned} \quad (23)$$

with boundary conditions (Fig. 9).

$$u_0 = u_n = 0; \beta_0 = \beta_n = 0; \beta_{-1} = -\beta_1; \beta_{n+1} = -\beta_{n-1} \quad (24)$$

The setting up of the finite difference equations at each pivotal point  $i = 1$  through  $i = n-1$  will give  $2(n-1)$  simultaneous equations in terms of  $(n-1)$  unknowns for  $u_i$  and  $\beta_i$  quantities each.

### III. DETERMINATION OF THE STIFFNESS PARAMETERS

The coefficients  $B_y$ ,  $C_T$ ,  $C_w$ ,  $P_{y_0}$  and  $\int_A \sigma s^2 dA$  occurring in the two finite difference equations are constant only as long as the member remains elastic. With yielding these coefficients change their value, and since yielding is a function of the bending moment distribution along the length of the member, these coefficients will not be the same at every point for which the finite difference equations are written. The coefficients can be thought of as cross-sectional properties, and they are fully defined if the distribution of the yielded zones at every cross section is known. Because of the presence of a secondary moment (axial force times deflection), the bending moment distributions and thus the inelastic zones are not known at the onset of lateral-torsional buckling.

The solution of the problem is therefore one of trial and error. For a given beam-column an axial force and an end moment is specified first, and the corresponding deflected shape and moment diagram is computed. It is now possible to determine the inelastic regions, and from this knowledge the coefficients of the two finite difference

equations are calculated at the distinct points for which these equations are written. If the originally chosen combinations of  $P$  and  $M_0$  are also the critical combinations for the start of lateral-torsional buckling, then the determinant of the coefficients of the  $2(n-1)$  finite difference equations is equal to zero. This will usually not occur at the first trial, and several values of  $M_0$  for a constant value of  $P$  are tried until one correct answer is obtained.

The analytical process of the solution of the problem is outlined in the block diagram of Fig. 10. The various steps, which will subsequently be discussed in more detail, are as follows:

- (1) Establish the moment-curvature-thrust ( $M-\theta-P$ ) relationships about the strong axis of the given wide-flange cross section and for the material properties.
- (2) Determine the moment-thrust-versus-yielded pattern relationships ( $M, P$ , vs.  $\alpha, \gamma, \psi, \nu$ ); where  $\alpha, \gamma, \psi$  and  $\nu$  represent the extent of yielding in the flanges and in the web, as shown in Fig. 11).



- (3) Establish the yielded pattern versus  $B_y$ ,  $C_w$ ,  $P_{y0}$ ,  $C_T$  and  $\int_A \sigma_s^2 dA$  relationships.
- (4) By combining the results of steps (2) and (3), determine the relationships between these coefficients and the axial force and the bending moment acting at any yielded cross section.
- (5) Construct the column deflection curve (CDC) by integration of the M- $\theta$ -P curves obtained in step (1) for a beam-column with specific values of P and  $M_0$ . The CDC gives the deflection and the moment at evenly spaced intervals along the length of the member.
- (6) The appropriate coefficients from step (4) are selected for the CDC from step (5) and the finite difference equations are set up.
- (7) The value of the determinant is tested in this step. If it is equal to zero, one point on the desired critical axial thrust - end moment - length curves is established; if it is not, a new CDC is chosen and the process is repeated until a correct answer is obtained.

### Moment-Curvature-Thrust Relationships

The determination of the M- $\phi$ -P curves is accomplished by assuming a specific stress distribution, and thus a yield pattern, and then computing the corresponding values of P, M, and  $\phi$  from geometry and equilibrium, (16) <sup>Ketter, Kawinsky, Beedle</sup> that is,

$$P = \int_A \sigma dA \quad ; \quad M = \int_A \sigma y dA \quad ; \quad \phi = \frac{\epsilon_1 - \epsilon_2}{d} \quad (25)$$

where  $\epsilon_1$  and  $\epsilon_2$  are the strains at the extreme fibers of the cross section.

As the moment is increased under a constant axial force, yielding will commence at the tips of the compression flange, since at these locations the compressive residual stress is maximum. As M is increased, yielding will penetrate through this flange. Eventually yielding occurs in the tension flange and in the web, and finally full plastification of the cross section results.

The non-dimensionalized  $\frac{M}{M_y} - \frac{\phi}{\phi_y} - \frac{P}{P_y}$  relationships about the strong axis have been determined for the following five different stages of yielding in the wide-flange section containing residual stresses:

- (1) Elastic case (Fig. 11a);
- (2) Partial yielding in the compression flange,

with yielding progressing from the flange tips towards the center while the web and the tension flange remain elastic (Fig. 11b);

- (3) Partial yielding in the compression flange, in the tension zone of the web, and in the tension flange (Fig. 11c);
- (4) Partial yielding in the compressed part of the web, while the remainder of the web and the tension flange are elastic and the compression flange is fully plastic (Fig. 11d);
- (5) Partial yielding in both the compression and tension zones of the web, and full plasticity in the compression and tension flanges (Fig. 11e).

The five patterns enumerated above do not include all the stages of yielding, but they permit the construction of the  $M-\phi$ - $P$  curves over the ranges of importance. Equations corresponding to four of the five yield patterns shown in Fig. 11 are listed in Table 1.

The  $M-\phi$ - $P$  relations can be presented as a family of curves, with  $M/M_y$  as the ordinate and  $\phi/\phi_y$ , as the abscissa.

Each curve is for a constant value of  $P/P_y$ . Such curves are shown in Fig. 12 for the 8WF31 shape and for  $E = 30,000$  ksi;  $\sigma_y = 33$  ksi; and  $\sigma_{rc} = 0.3\sigma_y$ . Also shown on the curves in Fig. 12 are the regions where the various patterns of yielding given in Fig. 11 occur. Patterns b) and c) predominate for the curve for  $P = 0$ , and patterns b) and d) are valid over a relatively wide range if  $P \geq 0.2P_y$ .

### Stiffness Parameters

The coefficients  $B_y$ ,  $C_T$ ,  $C_w$ ,  $P_{y0}$  and  $\int_A \sigma s^2 dA$  represent the instantaneous resistance of the member, which has been previously bent in the plane of the web and which may have already yielded in a pattern which is symmetric about the y-axis, to infinitesimally small lateral and torsional moments at the instant of lateral-torsional buckling.

The coefficients  $B_y$ ,  $C_T$  and  $C_w$  are the weak-axis bending stiffness, the St. Venant's torsional stiffness, and the warping torsional stiffness, respectively. The distance between the centroid of the unyielded section and the shear center of the elastic core is  $y_0$ , and the coefficient  $\int_A \sigma s^2 dA$  is an index of the torque contribution of the components of the stresses in the warped plane.

There are two ways for determining the values of the coefficients; (1) one might choose to consider the stiffness just prior to buckling, in which case previously yielded fibers offer no resistance (tangent modulus concept), or (2) one might consider the stiffness just after buckling, in which case elastic unloading of previously yielded fibers would increase the resistance (reduced modulus concept).<sup>(14)</sup> The first of these two methods is used in this report. Thus the stiffness parameters are computed for the elastic core.

a) Weak Axis Bending Stiffness,  $B_y$

The resistance to lateral bending is proportional to the stiffness  $B_y$ , and this is equal to the modulus of elasticity  $E$ , times the moment of inertia of the elastic core about the y-axis. The yielded portions are assumed to possess no stiffness, since in these regions  $E = 0$  (Fig. 2). The equations for  $B_y$  for the prevalent yield patterns are:

Pattern of Fig. 11b.

$$B_y = \left[ \frac{1 + (1 - 2\alpha)^3}{2} \right] EI_y \quad (26)$$

Pattern of Fig. 11c

$$B_y = \left[ \frac{1 + (1 - 2\alpha)^3 - 8\psi^3}{2} \right] EI_y \quad (27)$$

Pattern of Fig. 11e

$$B_y = \frac{1}{2} EI_y \quad (28)$$

In Eqs. (26) through (28),  $I_y$  is the moment of inertia of the full cross section.

b) St. Venant Torsional Stiffness,  $C_T$

The torsional stiffness  $C_T$  may be determined by applying an infinitesimal torque to the member which has already yielded by bending in the plane of the web. A relationship between the incremental changes of stress and strain in each element in the plastic zone is given by the Reuss equation as (17)(18)

$$\frac{d\gamma - \frac{d\tau}{G}}{d\varepsilon - \frac{d\sigma}{E}} = \frac{3\tau}{\sigma} \quad (29)$$

where  $d\sigma$ ,  $d\varepsilon$ , and  $d\tau$  and  $d\gamma$  are the incremental changes of stress and strain in normal and shear directions.

No shearing stress due to bending exists in the yielded portion of the cross section just prior to buckling (19). At the instant of the application of the infinitesimal torque thus,  $\tau = 0$ , and Eq. (29) reduces to

$$d\tau = G d\gamma \quad (30)$$

This equation is the same as the relationship which exists in the elastic fibers of the cross section, and thus the infinitesimal torque is resisted as if the whole member were

elastic. Therefore,

$$C_T = GK_T = \frac{G}{3} \left[ 2bt^3 + (d-2t)w^3 \right] \quad (31)$$

c) Warping Stiffness,  $C_w$

The warping stiffness  $C_w$  represents the resistance of the flanges of the member to cross bending. This resistance is provided by the elastic core of the flanges since in the yielded portions  $E = 0$ . The equations of  $C_w$  for the most prevalent cases of yielding are:

Pattern of Fig. 11b:

$$C_w = \left[ \frac{2}{1 + \frac{1}{(1-2\alpha)^3}} \right] EI_w \quad (32)$$

Pattern of Fig. 11c:

$$C_w = \left[ \frac{2(1-2\alpha)^3(1-8\psi^3)}{1 + (1-2\alpha)^3 - 8\psi^3} \right] EI_w \quad (33)$$

Pattern of Fig. 11d:

$$C_w = \frac{E}{288} \left[ 2b^3t^3 + \left\{ 2(1-\gamma)d-t \right\}^3 w^3 \right] \quad (34)$$

$I_w$  in Eqs. (32) and (33) is the warping moment of inertia of the whole cross section,

$$I_w = \frac{(d-t)^2}{4} I_y \quad (35)$$

d) Shear Center Distance,  $y_0$

The distance between the centroid of the unyielded cross section and the shear center of the elastic core is defined by the following equations:

Pattern of Fig. 11b:

$$y_o = \left[ \frac{(1-2\alpha)^3}{1+(1-2\alpha)^3} - \frac{1}{2} \right] (d-t) \quad (36)$$

Pattern of Fig. 11c:

$$y_o = \left[ \frac{(1-2\alpha)^3}{1+(1-2\alpha)^3 - 8\psi^3} - \frac{1}{2} \right] (d-t) \quad (37)$$

Pattern of Fig. 11d:

$$y_o = -\frac{1}{2} (d-t) \quad (38)$$

e) Coefficient,  $\int_A \sigma_s^2 dA$

The coefficient  $\int_A \sigma_s^2 dA$  of the equivalent torsional rigidity  $(C_T - \int_A \sigma_s^2 dA)$  in Eq. (19) is a reduction of the St. Venant's torsional stiffness due to the distributed stresses on the warped cross section at the instant when lateral instability occurs.

In the elastic range the value of this coefficient is

$$\int_A \sigma_s^2 dA = P \left( \frac{I_x + I_y}{A} \right) + \bar{C} \quad (39)$$

The term  $\bar{C}$  in this equation represents the contribution of the residual stresses, and it is equal to

$$\bar{C} = \frac{tb^3}{8} (\sigma_{rc} - \frac{\sigma_{rt}}{3}) + \frac{tb}{4} (d-t)^2 (\sigma_{rc} - \sigma_{rt}) - \frac{w}{12} (d-2t)^3 \sigma_{rt} \quad (40)$$

In the inelastic range  $\int_A \sigma_s^2 dA$  is expressed as the sum of the effects of the residual stresses and the stress



due to the axial force P and the bending moment M, that is

$$\int_A \sigma s^2 dA = \left[ \int_A \sigma s^2 dA \right]_{R.S.} + \left[ \int_A \sigma s^2 dA \right]_{P+M} \quad (41)$$

For the prevalent cases of yielding, the equations of these coefficients are:

Pattern of Fig. 11b:

$$\begin{aligned} \left[ \int_A \sigma s^2 dA \right]_{R.S.} &= \frac{b^3 t}{8} (\sigma_{rc} - \sigma_{rt}) + \frac{bt}{2} (d-t)^2 (\sigma_{rc} - \sigma_{rt}) \left[ \left\{ 1 - \frac{1}{1+(1-2\alpha)^3} \right\}^2 \right. \\ &+ \left. \left\{ \frac{1}{1+(1-2\alpha)^3} \right\}^2 \right] - \frac{W}{3} (d-t)^3 \sigma_{rt} \left[ \left\{ 1 - \frac{1}{1+(1-2\alpha)^3} - \frac{t}{2(d-t)} \right\}^3 \right. \\ &+ \left. \left\{ \frac{1}{1+(1-2\alpha)^3} - \frac{t}{2(d-t)} \right\}^3 \right] \end{aligned} \quad (42)$$

$$\begin{aligned} \left[ \int_A \sigma s^2 dA \right]_{P+M} &= bt \sigma_1 \left[ \frac{b^2}{6} + (d-t)^2 \left[ \left\{ 1 - \frac{1}{1+(1-2\alpha)^3} \right\}^2 + \left\{ \frac{1}{1+(1-2\alpha)^3} \right\}^2 \right] \right] \\ &- bt \sigma_y \frac{\phi}{\phi_y} \left[ \frac{b^2}{6} + 2(d-t)^2 \left\{ 1 - \frac{1}{1+(1-2\alpha)^3} \right\} \right] - 2\alpha^2 bt (\sigma_{rc} + \sigma_{rt}) \left\{ \frac{d-t}{1+(1-2\alpha)^3} \right\}^2 \\ &- \frac{b^3 t}{6} \alpha^2 (\sigma_{rc} + \sigma_{rt}) (3 - 4\alpha + 2\alpha^2) + \frac{W \sigma_y \phi}{2d \phi_y} (d-t)^4 \left[ \left\{ \frac{1}{1+(1-2\alpha)^3} - \frac{t}{2(d-t)} \right\}^4 \right. \\ &- \left. \left\{ 1 - \frac{1}{1+(1-2\alpha)^3} - \frac{t}{2(d-t)} \right\}^4 \right] + \frac{W}{3} (d-t)^3 \left[ \sigma_1 - 2\sigma_y \frac{\phi}{\phi_y} \left( 1 - \frac{t}{d} \right) \right] \left\{ \frac{1}{1+(1-2\alpha)^3} \right\} \\ &+ \left. \frac{t}{2(d-t)} \right\} \left[ \left\{ 1 - \frac{1}{1+(1-2\alpha)^3} - \frac{t}{2(d-t)} \right\}^3 + \left\{ \frac{1}{1+(1-2\alpha)^3} - \frac{t}{2(d-t)} \right\}^3 \right] \end{aligned} \quad (43)$$

where  $\sigma_1 = \sigma_y - \sigma_{rc} + 2\alpha (\sigma_{rc} + \sigma_{rt})$

Pattern of Fig. 11c:

$$\int_A \sigma_s^2 dA = \text{Eq. (42)} + \text{Eq. (43)} + 2\psi^2 bt (\sigma_{rc} + \sigma_{rt}) \left\{ \frac{\psi^2 b^2}{6} + \left( k + \frac{t}{2} + \nu d \right)^2 \right\} + \frac{w \sigma_y \phi}{d \phi_y} \left\{ \frac{k^3}{6} + (k + \nu d) \left( \frac{\nu d}{2} - \frac{k}{6} \right) \right\} \quad (44)$$

$$\text{where } k = \frac{(1-2\alpha)^3}{1+(1-2\alpha)^3-8\psi^3} (d-t) - \frac{t}{2} - \nu d$$

Pattern of Fig. 11d:

$$\int_A \sigma_s^2 dA = \sigma_y \left\{ bt(d-t)^2 + \frac{wd^3}{3} \left( 1 - \frac{3t}{2d} \right)^3 + \frac{bt^3}{6} \right\} + \frac{bt^3}{16} (\sigma_{rc} + \sigma_{rt}) - \frac{\sigma_y \phi}{6 \phi_y} \left( 1 - \gamma - \frac{t}{2d} \right) \left\{ bt^3 + d^3 w \left( 1 - \gamma - \frac{t}{2d} \right)^3 \right\} \quad (45)$$

Equations (26) through (45) permit the calculation of the values of the pertinent coefficients appearing in the finite difference equations if the sectional and material properties as well as the yielding penetrations are specified. Since for these same yield patterns the corresponding moment and axial force are also known from the previous step where the M- $\phi$ -P relationships were computed, it is possible to combine these results and set up families of curves where each curve gives the correlation between any of the coefficients and the moment for constant values of P/P<sub>y</sub>. Such curves are shown for the 8WF31 shape in Figs. 13 through 16

for values of  $P/P_y = 0, 0.2, 0.4$  and  $0.6$ ; Fig. 13 gives the curve  $M/M_y$  versus  $C_w/C_T$ ; the curves  $M/M_y$  versus  $y_0/d$  are illustrated in Fig. 15; and finally the curves in Fig. 16 give the relationship between  $M/M_y$  and  $1 - \frac{\int_A s^2 dA}{C_T}$ . These curves are shown here to illustrate the variation of the coefficients in the inelastic range. In the elastic range the coefficients are constant.

The availability of such curves as shown in Figs. 13 through 16 would permit the determination of the required cross-sectional properties for any given value of the moment and the axial force. It should be pointed out that these curves represent an intermediate step in the calculation, and they need not actually be constructed, since the calculations represent a subroutine of the total digital computer program.

#### IV. LATERAL-TORSIONAL BUCKLING STRENGTH

##### Column Deflection Curves

The relationships discussed in the previous part of this paper are sectional properties; they must still be tied in with the actual problem to be solved. This is done with the aid of the column deflection curves (CDC-s). A CDC is the shape that a compressed member will assume if it is held in a bent configuration by axial loads applied at its ends. (20) (21) Any real beam-column deflected in the plane of symmetry can be thought of being part of such a CDC.

Two CDC-s are shown in Fig. 17a. The axial force  $P$ , applied at the two column ends, holds the member in a deflected shape. Since the bending moment at any point within the curves is proportional to the deflection, the deflection curve can also represent the moment diagram. The length in the CDC-s of Fig. 17 is non-dimensionalized as the strong axis slenderness ratio  $L/r_x$ , and all deformations take place in the plane of the paper.

There are an infinite number of possible CDC-s for any given symmetric cross section and a specified constant

axial force  $P$ . These various curves are differentiated from each other by the slope  $\theta_0$  at the end of the column.

The relationship between the beam-columns treated in this paper (axial force  $P$  and moment  $M_0$  at one end only) and the CDC-s is illustrated by Figs. 17b and c. The pinned end of the beam-column coincides with the end of the CDC. The other end of the beam-column is situated a distance equal to its length from the end of the CDC. The moment at this end is equal to the end moment  $M_0$ .

There are an infinite number of CDC segments which can be placed on the beam-column length for any given axial force and length. One of these segments will correspond to the maximum end moment  $M_{02MAX}$  (see Fig. 1) which the member can sustain if failure occurs by excessive bending in the plane of the applied moments (20) (21), and another one will correspond to the end moment  $M_{0CR}$  at which lateral torsional buckling is imminent. As shown in Fig. 17b and c, there are two CDC-s which have  $M_{0CR}$  as their end moment: One (Fig. 17b) is located on the ascending branch of the in-plane  $M-\theta$  curve in Fig. 1, and the other (Fig. 17c) is located on the descending branch. Of these two, only the first is of interest here.

The column deflection curves are obtained from the M- $\phi$ -P curves by numerical integration, (20) giving the value of the deflection, the slope, the moment and the curvature, as well as the yielded pattern, at evenly spaced discrete points along their whole lengths. From this knowledge it is then possible with the aid of Eqs. (26) through (45) to compute the stiffness coefficients.

#### Computational Procedures

The complete calculations from the M- $\phi$ -P curves to the setting up of the determinant of the coefficients of the finite difference equations were performed by a Royal McBee LGP-30 digital computer, and the process of calculation for one particular problem was essentially as follows:

- (1) An 8WF31 section of A7 steel was chosen as the member. The input into the computer consisted of the cross-sectional dimensions  $b$ ,  $d$ ,  $t$ , and  $w$ , and of the material properties  $\sigma_y = 33$  ksi,  $\sigma_{rc} = 0.3 \sigma_y$ ,  $E = 30,000$  ksi and  $G = 11,500$  ksi.
- (2) Next an axial force and a length was chosen.  
The following values of  $P$  were selected:  $0.2P_y$ ,

$0.4P_y$  and  $0.6P_y$ . The length was usually selected to be a multiple of  $2r_x$  or  $3r_x$ , since this has been shown to be a spacing resulting in adequate accuracy. (20)

- (3) From the input of step (1) above and for the specified axial force the  $M-\theta$  curve was computed.
- (4) Several CDC-s having different end slopes  $\theta_0$  were computed by numerical integration from the  $M-\theta$  curve of step (3).
- (5) One of the CDC-s, with a reasonable value of  $\theta_0$  was selected from the curves of step (4). (This initial choice of  $\theta_0$  will be discussed later). With  $P/P_y$  and  $\theta_0$  known, the value of  $M_0/M_y$  for the length  $L/r_x$  was determined from the CDC. Within the length of the beam-column, the moment and the curvature were also known at evenly spaced points.
- (6) Knowledge of the moment, curvature and axial force at these points also includes knowledge

of the distribution of the yielded zones (step (3) above), and from this the values of the sectional properties were computed at each point (Eqs. (26) through (45)).

- (7) The final results of this computational routine are the coefficients for the finite difference equations, and the axial force, length, and the end-moment of the beam-column.

The steps outlined above were computed in one continuous operation with one digital computer (LGP-30). The next step, that of calculating the value of the determinant of the coefficients, was performed by a larger computer and this operation is described next.

#### Characteristic Determinants

The setting up of the finite difference equations (Eqs. (22) and (23) with the boundary conditions of Eq. (24) at each pivotal point  $i = 1$  through  $i = n - 1$  gave  $2(n - 1)$  simultaneous equations in terms of  $(n - 1)$  unknowns  $u_i$  and  $\beta_i$  quantities each. This set of simultaneous equations may be written in matrix notation as

$$[A] \begin{Bmatrix} u \\ \beta \end{Bmatrix} = 0 \quad (46)$$



In this equation the matrix  $[A]$  is a set of the coefficients  $A_{ij}$  representing non-dimensional combinations of the cross-sectional properties ( $B_y$ ,  $C_w$ ,  $C_T$ ,  $P_{y_0}$ , and  $\int_A \sigma s^2 dA$ ), the load parameters ( $P$  and  $M_0$ ), and the length of the member. If the value of the determinant  $|A|$  is equal to zero, then the assumed combination of  $P$ ,  $M_0$ , and  $L$  is one which causes the bifurcation of the equilibrium, that is, the start of lateral-torsional buckling.

### Buckling Strength

Usually it was not possible to estimate the critical combination of  $P$ ,  $M_0$  and  $L$  such that  $|A| = 0$  at the first trial. Several values of  $M_0$  were tried for given constant values of  $P$  and  $L$ , and the final correct answer was obtained by interpolation. The initial choice of  $M_0$  was made easier by the existence of known upper and lower bounds. The upper bound was determined from the fact that  $M_{0CR}$  could not be larger than the end moment corresponding to failure by excessive bending in the plane of the applied moments ( $M_{02MAX}$  in Fig. 1).<sup>(3)</sup> A lower bound was provided by the knowledge that the most severe loading condition exists when two equal end moments cause the member to be bent in single

curvature deformation. Since inelastic lateral-torsional buckling solutions for this case were available, the lowest possible value of  $M_{OCR}$  could be found. (4)

The upper and lower bounds furnish two envelopes between which the true answer must lie. These envelopes are shown as heavy dashed lines in Fig. 18. This figure illustrates the various relationships which were involved in the solution of the problem. The curves are all for the 8WF31 shape bent about its strong axis, and they are for a constant axial load of  $0.2P_y$ .

The heavy lines (dashed and solid) in this figure represent the curves of end moment  $M_o/M_y$  as the ordinate versus the length of the member  $L/r_x$  as the abscissa. The upper dashed line gives the upper bound envelope for the case of a beam-column subjected to one end moment only and failing by excessive bending. At the right end this envelope is intersected by another dashed line which originates at  $L = 124r_x$  when  $M_o = 0$ , and this curve represents elastic lateral-torsional buckling as modified by the residual stresses. The terminal point of this curve at  $M_o = 0$  corresponds to weak-axis buckling under axial load only.

The lower dashed line is for the critical moment under equal end moments (lower bound) if failure is due to lateral torsional buckling. The terminal points of this curve are the critical weak axis buckling length  $l_{24r_x}$  when  $M_0 = 0$ , and the moment corresponding to full plastification for  $L = 0$ .

The heavy solid line in Fig. 18 represents the solution to the problem discussed in this paper. The circled points are the critical moments which were computed by trial and error.

Also shown in this figure are several column deflection curves (light solid lines) having various initial slopes  $\theta_0$ . The values of all the necessary coefficients in the determinant  $|A|$  are known at discrete points (marked points 0 to 16) along these CDC-s from the previous calculations.

The determination of a point on the critical  $M_0$ - $L$  curve is achieved by the following procedure for  $L = 48r_x$ : The value of the determinant  $|A|$  is determined for several CDC-s which terminate at  $L = 48r_x$  between the upper and the

lower bound envelopes. In this particular case the computations were made for the CDC-s having end slopes  $\theta_0$  between 0.07 and 0.09 radians. The critical point is obtained by linear interpolation of the values of the determinant  $|A|$ , as shown for the case of  $P = 0.2P_y$  in Fig. 19. For  $L = 48r_x$ , for example, five CDC-s were tried, and it can be seen that the value of  $|A|$  equals zero at  $M = 0.88M_y$ . The computation of all other points was performed in a similar manner. Curves of  $|A|$  versus  $M_0/M_y$  are shown in Fig. 19 for  $L = 96r_x$ ,  $64r_x$  and  $48r_x$ .

The M-L curves showing the final results, that is the curves for failure by excessive bending (upper light curve) for lateral-torsional buckling with one end moment (heavy curve), and for lateral-torsional buckling with two end moments (lower light curve) are shown in Figs. 20, 21 and 22, for  $P = 0.2P_y$ ,  $P = 0.4P_y$ , and  $P = 0.6P_y$ , respectively. These curves show that lateral-torsional buckling can indeed reduce the strength of beam-columns considerably in the inelastic range.

The final step in the computation, that is, the determination of the value of the determinant  $|A|$  was per-

formed with an IBM 7074 computer. For each specific beam-column length the spacing of the pivotal points on the CDC-s was chosen such that the final matrix always resulted in a 30 x 30 array of numbers. The number of pivotal points within the span was thus always equal to 15.

## V. SUMMARY

This report illustrates how the lateral-torsional buckling strength of as-rolled steel wide-flange beam-columns may be determined for buckling in the inelastic range. The report was intended to provide the theoretical background, the derivations of the equations, and the method of solution. A future report will discuss the significance of the results, the effects of the variation of the cross-sectional and material properties, and the loading condition. This future report will also include the comparison of the results of the theoretical work with the results of beam-column experiments, and empirical design formulas will be examined in the light of the theory presented here.

The following is a summary of the work reported in this paper:

- (1) The differential equations of lateral-torsional buckling are derived in a general form such that they express elastic as well as inelastic buckling. For elastic buckling the coefficients of the differential equations are constant, whereas

in the inelastic range these coefficients vary as the pattern of yielding.

- (2) The variation of the coefficients of the differential equations is determined for the various patterns of yielding which exist in wide-flange shapes containing residual stresses. Formulas and curves are presented to give the relationship between the axial force and bending moment and the resulting stiffness parameters.
- (3) The method of solution is illustrated by solving for the lateral-torsional buckling strength of beam-columns with simply supported ends and with moment applied at one end of the member. Since the moment, as well as the stiffness parameters, varies along the length of the member, the differential equations are solved by finite differences.
- (4) Critical combinations of length, axial force, and end moment are obtained by a trial and error procedure. The resulting interaction curves are shown in Figs. 20 through 22 for an ASTM A7 steel

8WF31 member. All computations were performed on digital computers.



## VI. ACKNOWLEDGEMENTS

This study is part of a general investigation "Welded Continuous Frames and Their Components" currently being carried out at the Fritz Engineering Laboratory of the Civil Engineering Department of Lehigh University under the general direction of Lynn S. Beedle. W. J. Eney is head of the Civil Engineering Department and the head of Fritz Engineering Laboratory. The investigation is sponsored jointly by the Welding Research Council, and the Department of the Navy, with funds furnished by the American Institute of Steel Construction, the American Iron and Steel Institute, Lehigh University Institute of Research, the Office of Naval Research, the Bureau of Ships, and the Bureau of Yards and Docks. The Column Research Council acts in an advisory capacity.

The authors wish to express their appreciation to Mr. Marshall Warner of IBM in Bethlehem, Pennsylvania for his help in the computation of the buckling determinant by the IBM 7074 computer.

VII. NOTATIONS

A	Area of cross section
$A_{ij}$	Cross-sectional coefficient in finite difference equation
$ A $	Determinant of cross-sectional coefficients
$[A]$	Square matrix of cross-sectional coefficients
$B_x$	Bending stiffness about x-axis (strong axis stiffness)
$B_y$	Bending stiffness about y-axis (weak axis stiffness)
b	Flange width
$C_T$	St. Venant torsional stiffness
$C_w$	Warping stiffness
$\bar{C}$	Modified torsional stiffness due to the effect of residual stress
d	Depth of section
E	Young's modulus of elasticity
$e_{yB}$	Smaller of the two end eccentricities
$e_{yT}$	Larger of the two end eccentricities
G	Modulus of elasticity in shear
h	Distance between pivotal points
$I_w$	Warping constant
$I_x, I_y$	Moments of inertia about the x and y axis, respectively

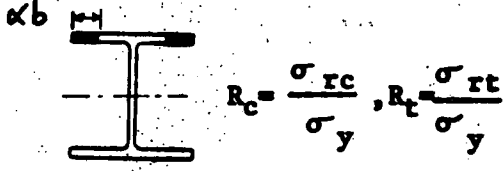
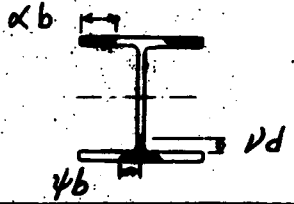
$K_T$	St. Venant torsional constant
$L$	Length of beam-column
$M$	Bending moment
$M_o$	Applied end bending moment
$M_{OCR}$	End bending moment at which the beam-column buckles laterally
$M_{o1MAX}$	Maximum end bending moment due to lateral-torsional buckling
$M_{o2MAX}$	Maximum end bending moment at which the beam-column fails by excessive bending in the plane of applied end moment
$M_{pc}$	Plastic hinge moment modified to include the effect of axial thrust
$M_x, M_y$	Bending moment about x- and y-axis, respectively
$M_y$	Moment at which yielding first occurs in flexure $M_y = S \sigma_y$
$M_{\xi 1}, M_{\xi 2}, M_{\xi 3}, M_{\xi 4}$	Components of $M_y$
$M_{\xi}, M_{\eta}, M_{\zeta}$	Moment about $\xi$ , $\eta$ and $\zeta$ axis, respectively
$n$	Number of subdivisions
$o$	Location of centroid
$P$	Axial thrust
$P_y$	Axial load corresponding to yield stress level, $P_y = A \sigma_y$

$R_c, R_t$	$R_c = \sigma_{rc} / \sigma_y, R_t = \sigma_{rt} / \sigma_y$
$r_x, r_y$	Radius of gyration about x- and y-axis, respectively
S	Location of shear center
S	Section modulus about x-axis
s	Distance of any point on the cross section from shear center
t	Flange thickness
u, v	Displacement of shear center in x- and y-directions, respectively
$u_{i-1}, u_i, u_{i+1}$	Displacement u at each pivotal point, i-1, i, and i+1, respectively
w	Web thickness
x, y	Principal coordinates of the cross section
$y_0$	Distance between original centroid and shear center
z	Coordinate along undeformed beam-column center line
$\alpha$	Ratio of the width of yielding in compression flange to the flange width
$\beta$	Twisting angle at cross section about shear center
$\beta_{i-1}, \beta_i, \beta_{i+1}$	Twisting angle $\beta$ at each pivotal point, i-1, i, and i+1, respectively
$\gamma$	Shearing strain

$\gamma$	Ratio of the depth of yielding in compression web to the depth of cross section
$\epsilon_1, \epsilon_2$	Strains at both extreme fibers
$\theta$	Rotation at end of beam-column
$\theta_0$	Initial slope of column deflection curve
$\nu$	A coefficient indicating tensile yielding in the web
$\xi, \eta, \zeta$	Cartesian reference coordinates after displacement has taken place
$\beta$	Ratio of end bending moments
$\sigma$	Normal stress
$\sigma_{rc}, \sigma_{rt}$	Maximum compressive and tensile residual stress, respectively
$\sigma_y$	Yield stress level
$\tau$	Shear stress
$\phi$	Curvature
$\phi_y$	Curvature corresponding to first yield in flexure ( $\sigma_{rc} = 0$ )
$\psi$	A coefficient indicating yielding in the tension flange

VIII. TABLES AND FIGURES

TABLE 1 MOMENT - CURVATURE - THRUST RELATIONSHIPS

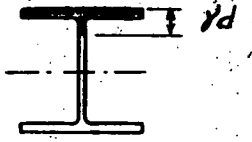

<p>Yield Patterns</p>	 <p><math>R_c = \frac{\sigma_{rc}}{\sigma_y}, R_t = \frac{\sigma_{rt}}{\sigma_y}</math></p>	 <p><math>\psi b</math></p>
<p>Given</p>	<p><math>P/P_y, \theta/\theta_y, b, d, t, w, E, \sigma_y, R_c, R_t</math></p>	<p><math>P/P_y = 0, \theta/\theta_y, b, d, t, w, E, \sigma_y, R_c, R_t</math></p>
<p>Limits</p>	$\frac{1}{R_c + R_t} \left( \frac{t}{d} \right) \left( \frac{\phi}{\phi_y} \right) \leq \alpha < \frac{1}{2}$ <p>(Assume no yielding in tension flange)</p>	$\alpha_1 \leq \alpha \leq \frac{1}{2}^*$ $\alpha_1 = \frac{1}{2} \left\{ m_1 - \sqrt{m_1^2 - 4n_1} \right\}$
<p>Yield Extensions</p>	$\alpha = \frac{A}{2bt} + \frac{1}{2(R_c + R_t)} \frac{t}{d} \frac{\phi}{\phi_y}$ $-\sqrt{\frac{A}{2bt} \left[ \frac{A}{2bt} + \frac{1}{R_c + R_t} \left\{ 1 - R_c - \frac{P}{P_y} - \left( 1 - \frac{t}{d} \right) \frac{\phi}{\phi_y} \right\} \right] - \frac{1}{12} \left\{ \frac{1}{R_c + R_t} \frac{t}{d} \frac{\phi}{\phi_y} \right\}^2}$	$\alpha = \frac{bt}{dw} \frac{\phi}{\phi_y} \left[ D + \sqrt{D^2 + \frac{2dw}{bt} \frac{R_c + R_t}{\phi_y} F} \right]^*$ $\psi = \frac{1}{R_c + R_t} \left( \frac{\phi}{\phi_y} - 1 \right) + \left( \frac{1}{2} - \alpha \right)$ $\nu = \psi (R_c + R_t) \frac{1}{\phi_y} - \frac{t}{d}$
<p>Bending Moment</p>	$\frac{M}{M_y} = \frac{\phi}{\phi_y} \left\{ 1 + \alpha \frac{tbd}{S} \left( \frac{t}{d} \right) \left( 1 - \frac{2t}{3d} \right) \right\}$ $- \frac{tbd}{S} \left\{ \frac{\left( \frac{t}{d} \right)^2 \left( 1 - \frac{2t}{3d} \right) \left( \frac{\phi}{\phi_y} \right)^2}{3(R_c + R_t)} + \alpha^2 \left( 1 - \frac{t}{d} \right) (R_c + R_t) \right\}$	$\frac{M}{M_y} = \frac{tbd}{S} \left[ \left( 1 - \frac{t}{d} \right) \frac{\phi}{\phi_y} - (R_c + R_t) (\alpha^2 + \psi^2) \right] - \frac{t\phi}{d\phi_y} \left( 1 - \alpha - \psi \right) - \frac{4t}{3d}$ $+ \frac{1}{R_c + R_t} \frac{\phi t}{\phi_y d} \left( \frac{2t}{3d} \right) + \frac{wd^2}{6S} \left[ 1 - (R_c + R_t) \left( \frac{1}{2} - \alpha \right) - \frac{t\phi}{d\phi_y} \right]$ $\left[ \left( 1 - \frac{2t}{d} \right)^2 + \nu \left( 1 - \frac{2t}{d} \right) - 2\nu^2 \right]$

\* 
$$D = \frac{2}{R_c + R_t} \left\{ \frac{\phi}{\phi_y} \left( 1 - \frac{t}{d} \right) - 1 \right\} + \frac{w}{2b} - \frac{1}{\phi_y} \frac{dw}{bt} \left( 1 - \frac{R_c + R_t}{2} \right) - 1$$

$$F = \frac{1}{(R_c + R_t) \left( \frac{\phi}{\phi_y} - 1 \right)} \left\{ 1 - \left( 1 - \frac{t}{d} \right) \frac{\phi}{\phi_y} \right\} + \frac{1}{2} \left( 1 - \frac{w}{b} \right) \left\{ 1 + \frac{t}{d} \frac{1}{R_c + R_t} \frac{\phi}{\phi_y} \right\} + \frac{dw}{2bt} \frac{1}{R_c + R_t} \left[ 1 - \frac{1}{\phi_y} \left( 1 - \frac{R_c + R_t}{2} \right) \right] - \frac{1}{4}$$

$$m_1 = \frac{1}{\frac{R_c + R_t}{d/t} - 2} + \frac{A}{2bt}, \quad n_1 = \frac{A}{2bt} \left[ \frac{d}{t} \left( \frac{1}{R_c + R_t} - \frac{1}{2} \right) - \frac{1 - R_c}{R_c + R_t} \left( \frac{d}{t} - 1 \right) \right] \frac{1}{d/t - 2}$$

TABLE 1 - CONTINUED

<p><b>Yield Patterns</b></p>		
<p><b>Given</b></p>	<p><math>P/P_y, \phi/\phi_y, b, d, t, w, E, \sigma_y, R_c, R_t</math></p>	<p><math>P/P_y, \phi/\phi_y, b, d, t, w, E, \sigma_y, R_c, R_t</math></p>
<p><b>Limits</b></p>	$\frac{t}{d} \leq \gamma \leq 1 - \frac{t}{d}$ $\frac{R_c + R_t}{2(1-\gamma)} \leq \frac{\phi}{\phi_y} \leq \frac{1}{1-\gamma}$	$\frac{t}{d} \leq \gamma_1 \leq 1 - \frac{t}{d}$ $\frac{t}{d} \leq \gamma_2 \leq 1 - \gamma_1$ <p>or <math>(1-\gamma_1) \frac{R_c + R_t}{2 + R_c + R_t} \leq \gamma_2 \leq 1 - \gamma_1</math></p>
<p><b>Yield Extensions</b></p>	$\gamma = 1 + \frac{t}{d} \left( \frac{b}{w} - 1 \right) - \sqrt{\frac{b}{w} \left( \frac{t}{d} \right)^2 \left( \frac{b}{w} - 1 \right) + \frac{A}{wd} \left( 1 + \frac{R_c}{2} - \frac{P}{P_y} \right) \frac{1}{\phi_y \phi_y}}$	$\gamma_1 = \frac{1}{2} \left[ \frac{A P}{wd \phi_y} + \frac{bt}{dw} R_c - \frac{1}{dw} (A - bt) R_t + 1 - \frac{1}{\phi_y \phi_y} \right]$ $\gamma_2 = 1 - \frac{1}{\phi_y \phi_y} - \gamma_1$
<p><b>Bending Moment</b></p>	$\frac{M}{M_y} = \frac{wd^2}{6S} \left( 1 - \gamma - \frac{t}{d} \right) \left( 1 + 2\gamma - \frac{4t}{d} \right) \frac{\phi}{\phi_y}$ $+ \frac{bdt}{S} \left[ \left\{ (1-\gamma) \left( 1 - \frac{t}{d} \right) - \frac{1}{2} \left( 1 - \frac{4t}{3d} \right) \frac{t}{d} \right\} \frac{\phi}{\phi_y} - \frac{1}{4} \left( 1 - \frac{t}{d} \right) (R_c + R_t) \right]$	$\frac{M}{M_y} = \frac{t(d-t)(b-w)}{S} + \frac{wd^2}{6S} \left[ 2 - \frac{1}{\phi_y \phi_y} - 2(\gamma_1 - \gamma_2)^2 - 2\gamma_1 \gamma_2 \right]$



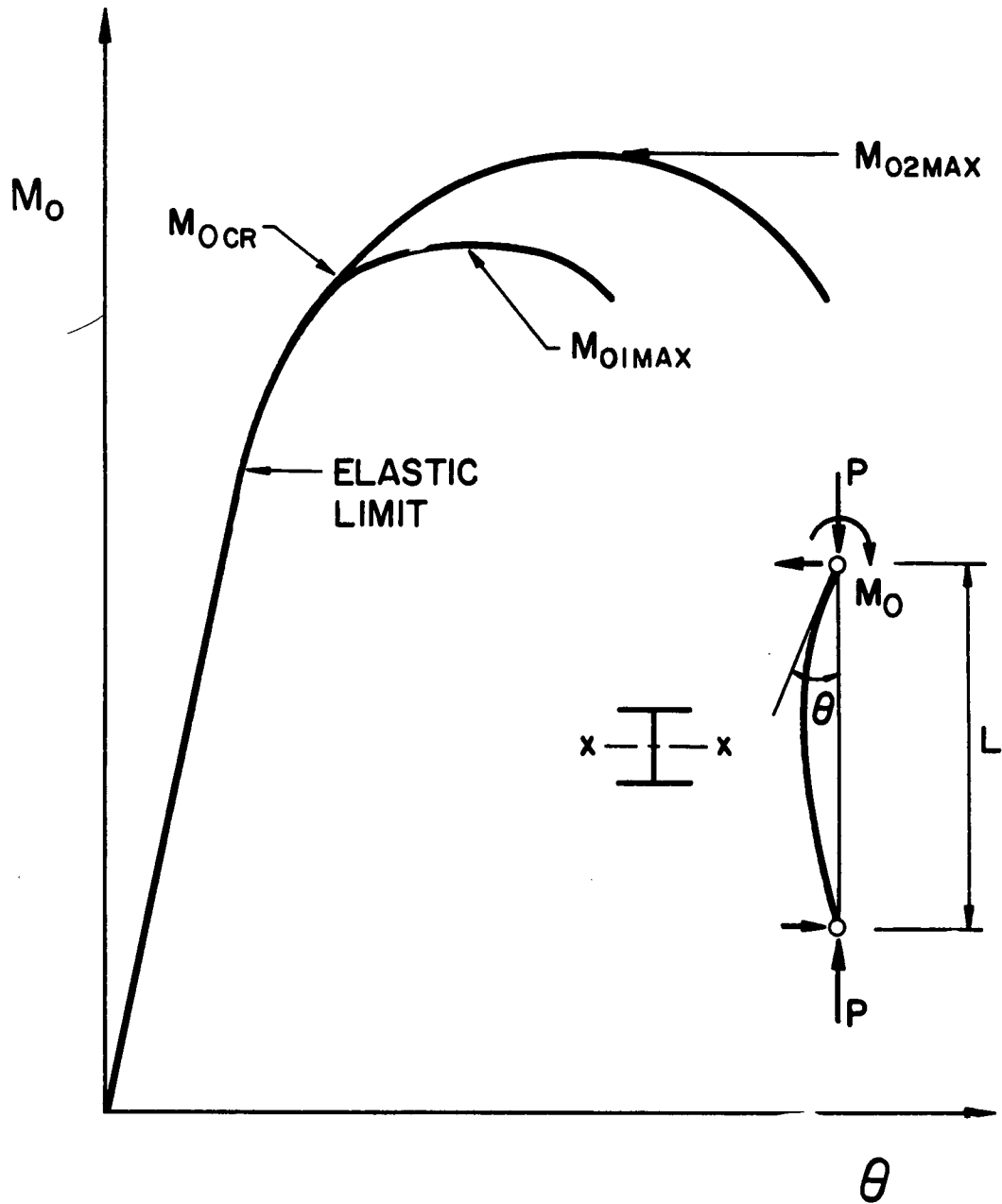


Fig. 1  $M_0$ - $\theta$  for Beam-Columns

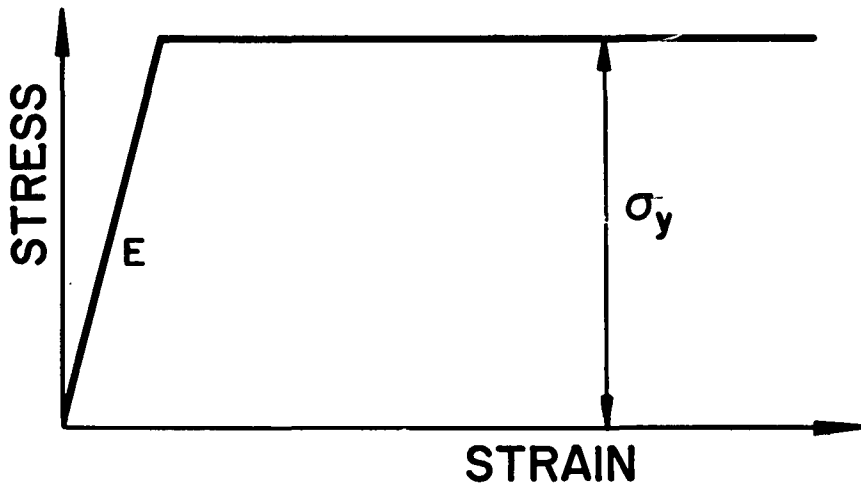


Fig. 2 Idealized Stress-Strain Diagram

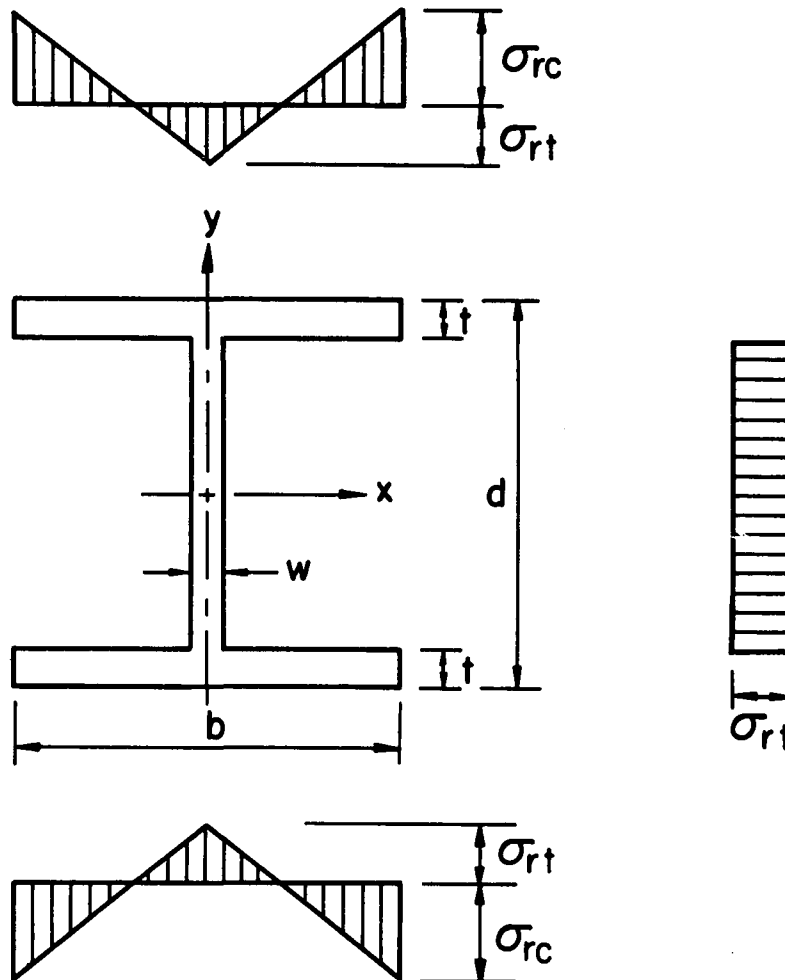


Fig. 3 Assumed Cooling Residual Stress Pattern

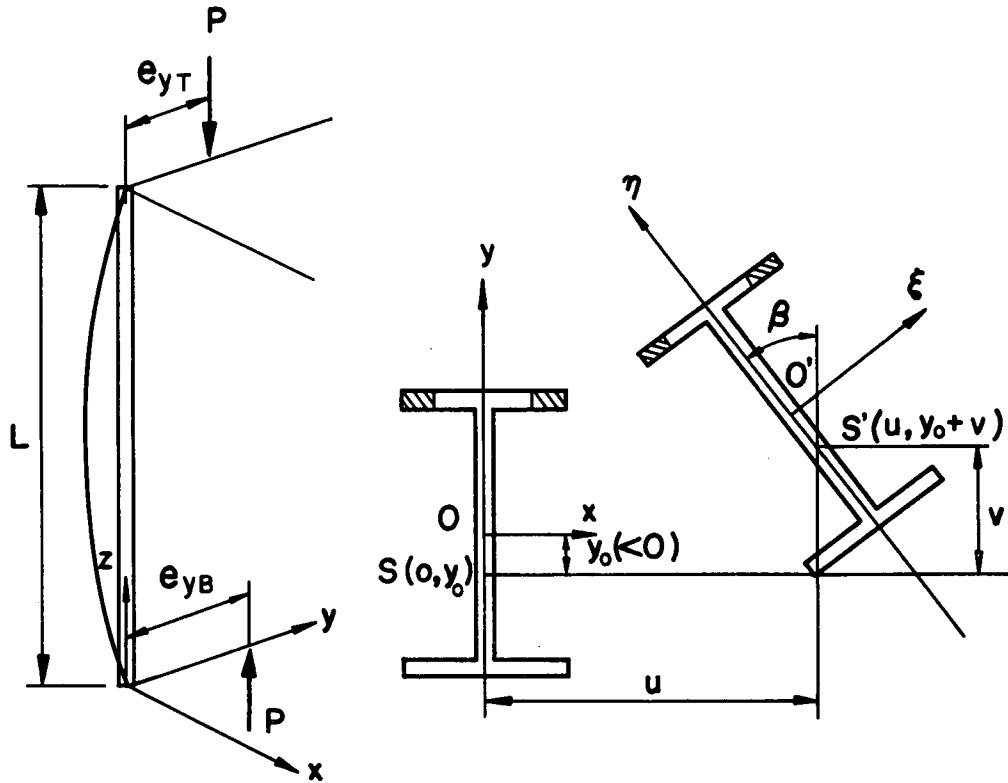


Fig. 4 Loading Condition and Properties of Cross Section

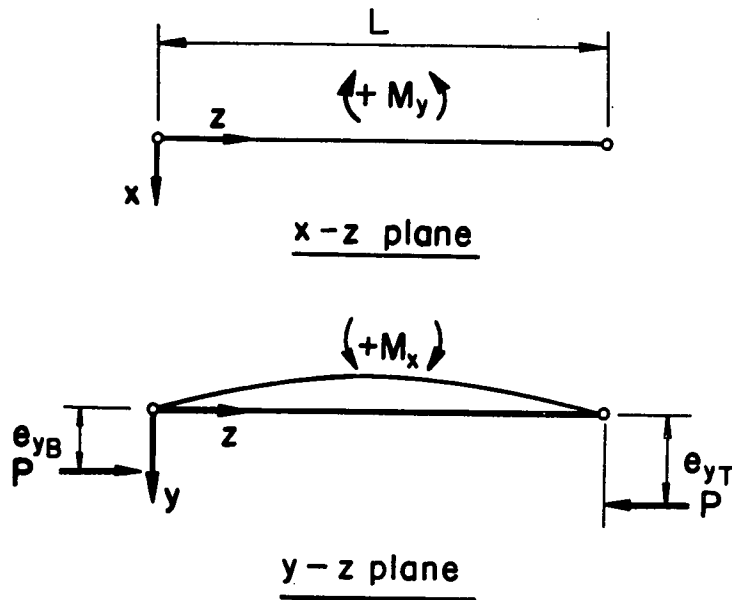


Fig. 5 Positive Directions of Bending Moments

205A.34

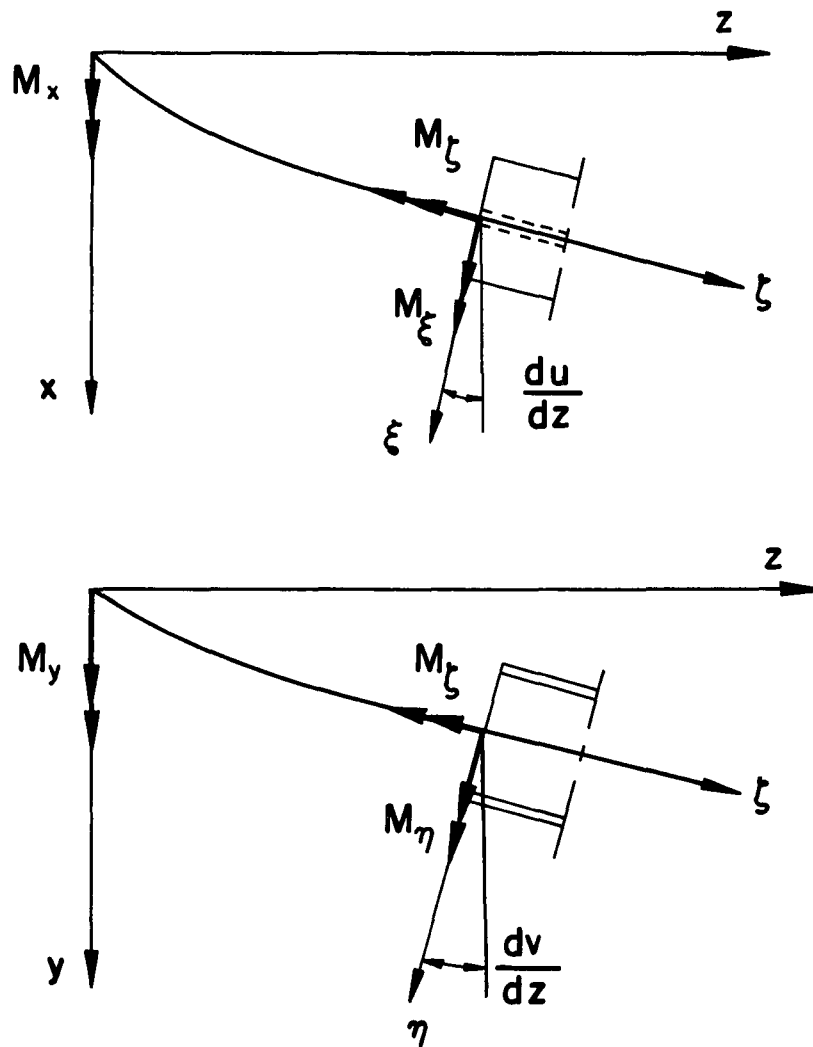


Fig. 6 Transformation of Moments to  $\xi, \eta, \zeta$  axes

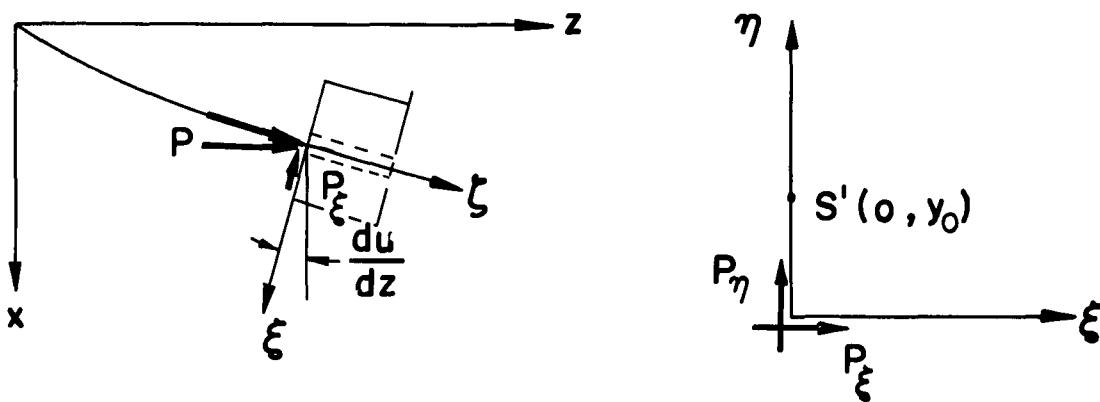


Fig. 7 Torque  $M_{\zeta 2}$  due to the Components of Axial Force  $P$

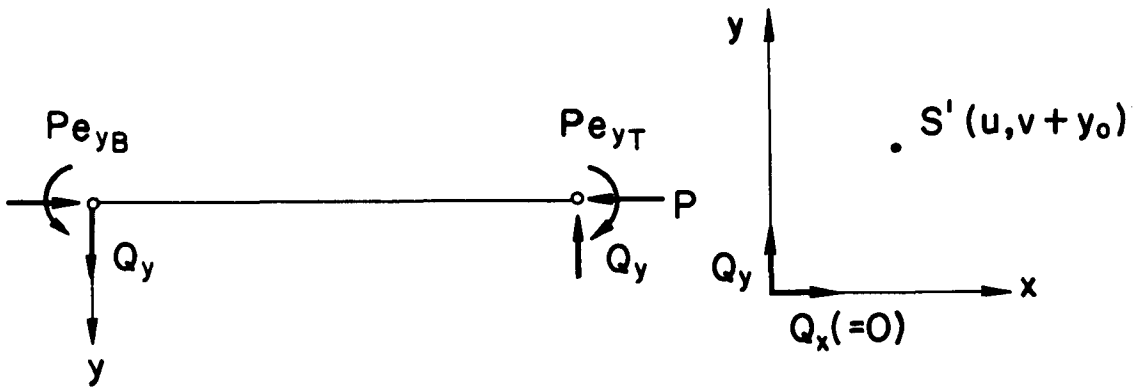


Fig. 8 Torque  $M_{S_4}$  due to the End Reactions  $Q_y$

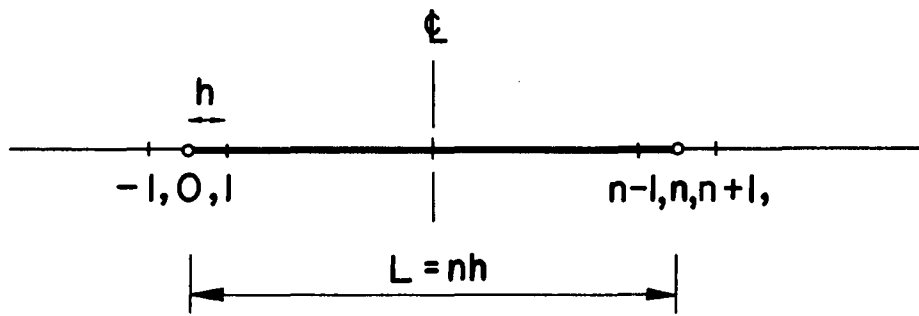


Fig. 9 Pivotal Points along the Beam Length

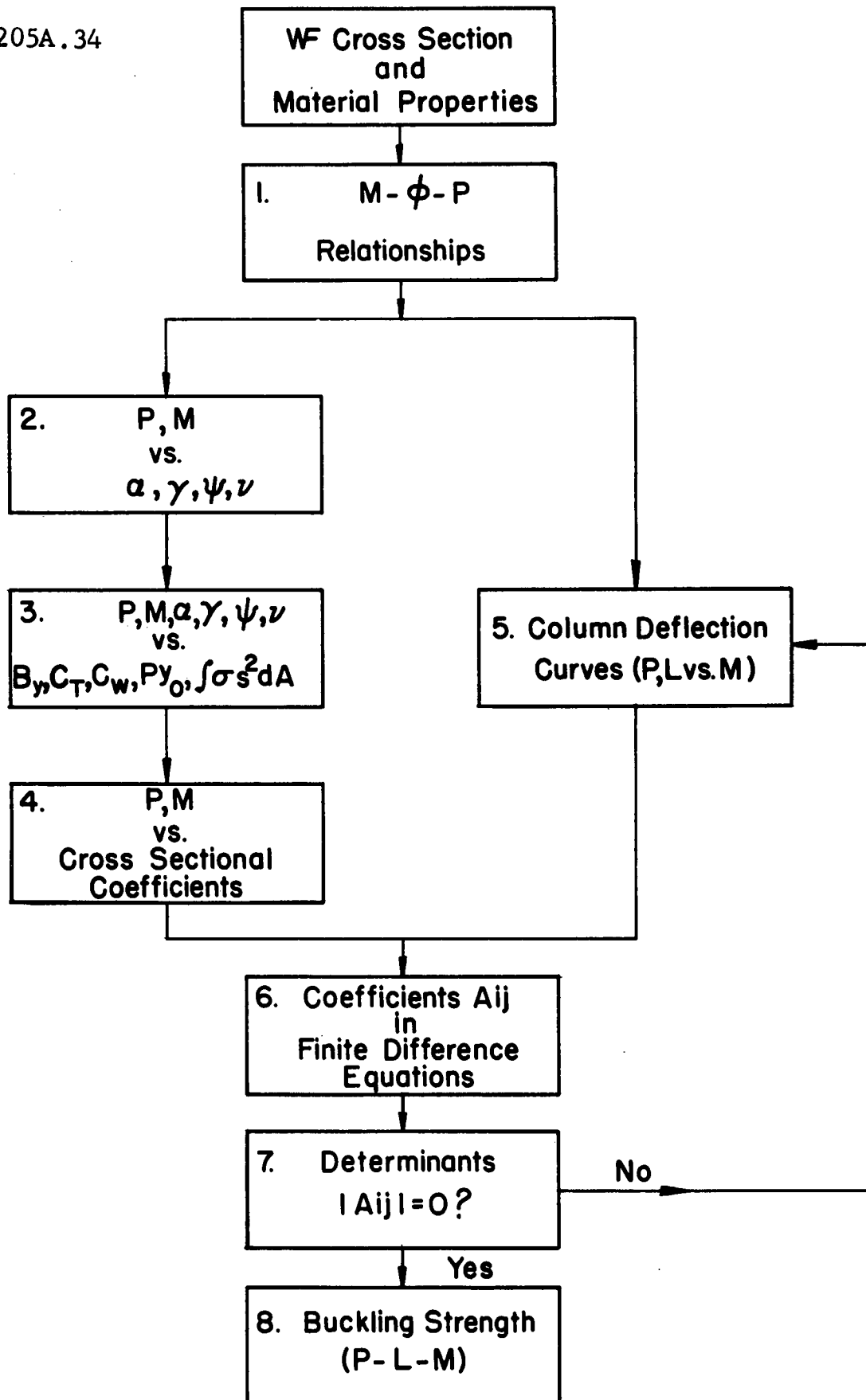


Fig. 10 Block Diagram for Computational Procedures

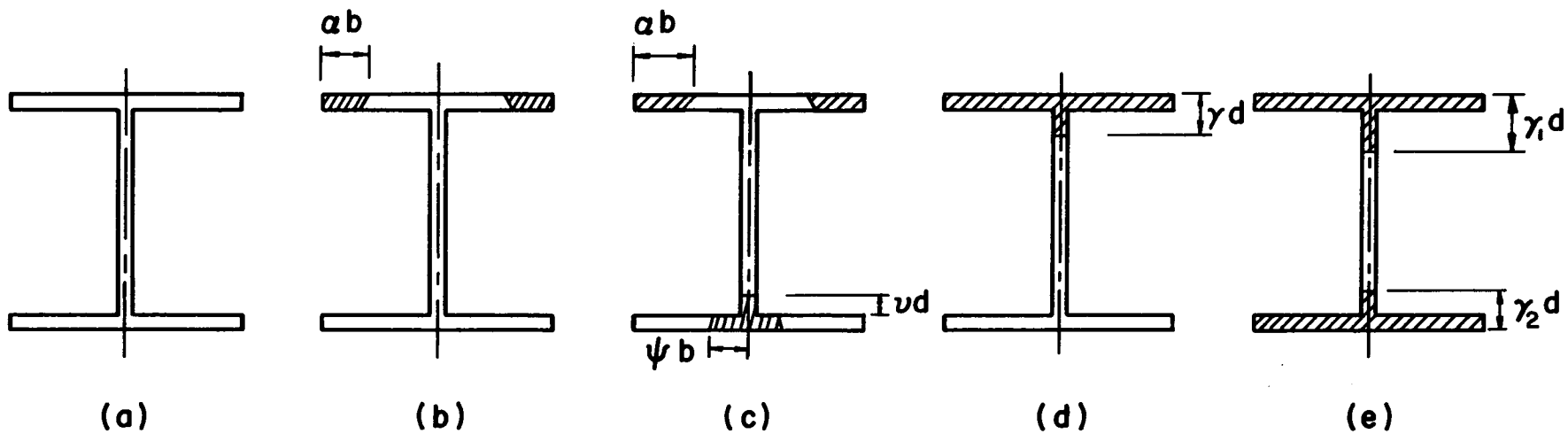


Fig. 11 Yield Patterns for Wide-Flange Cross Section

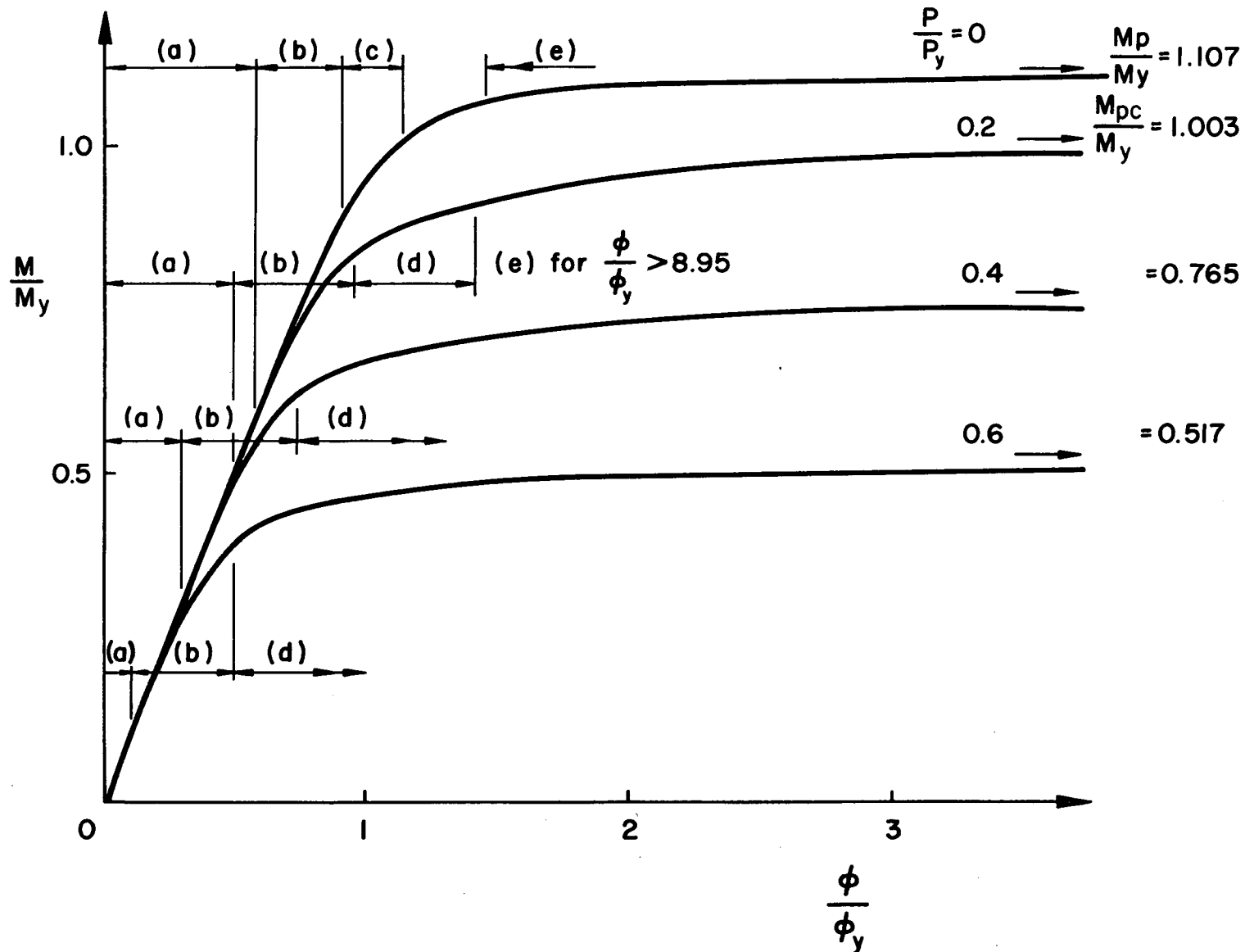


Fig. 12 Moment-Curvature-Thrust Relationships  
 for Strong Axis Bending, 8WF31,  $R_c = 0.3$



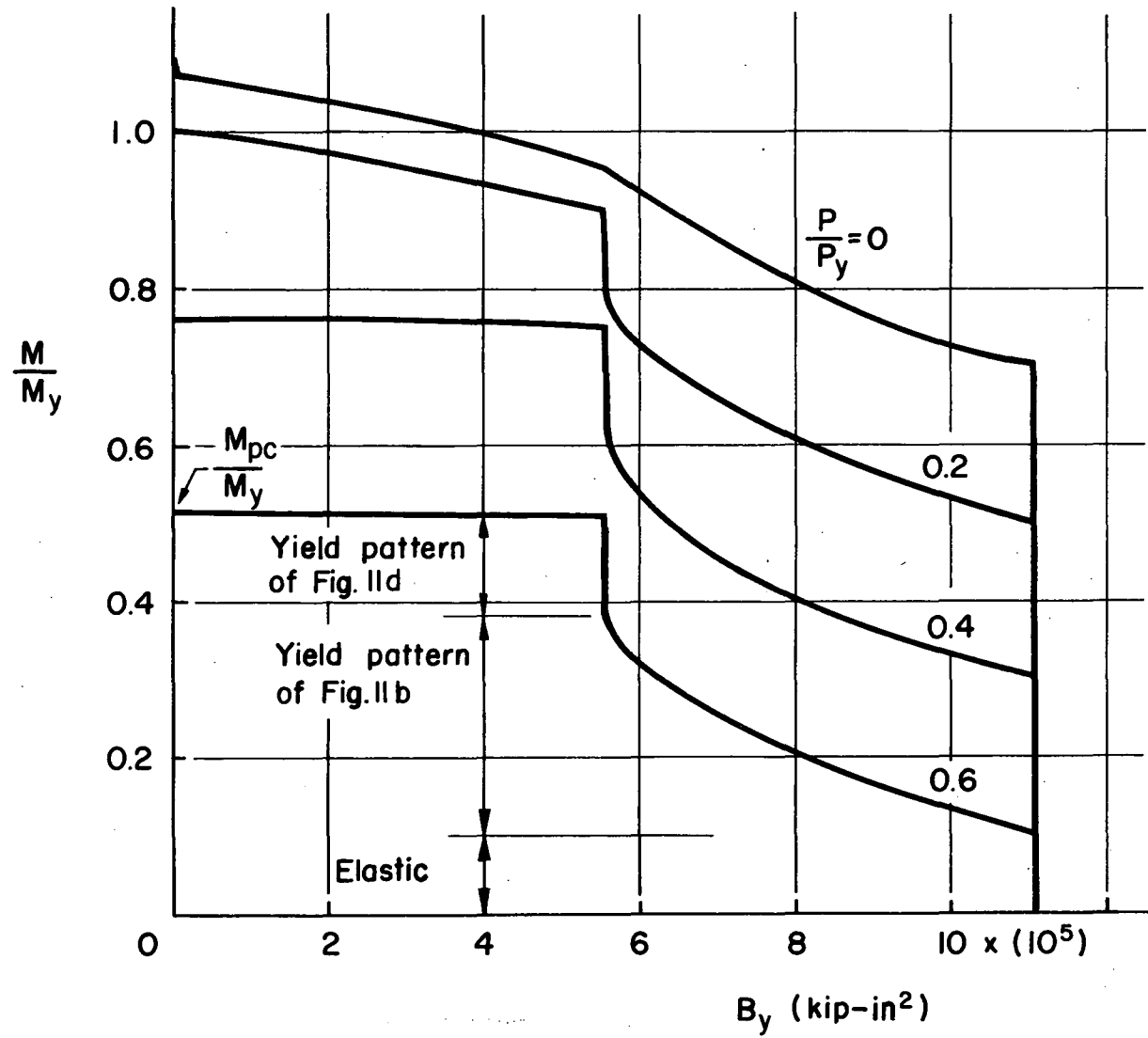


Fig. 13  $M/M_y$  versus  $B_y$  Curves

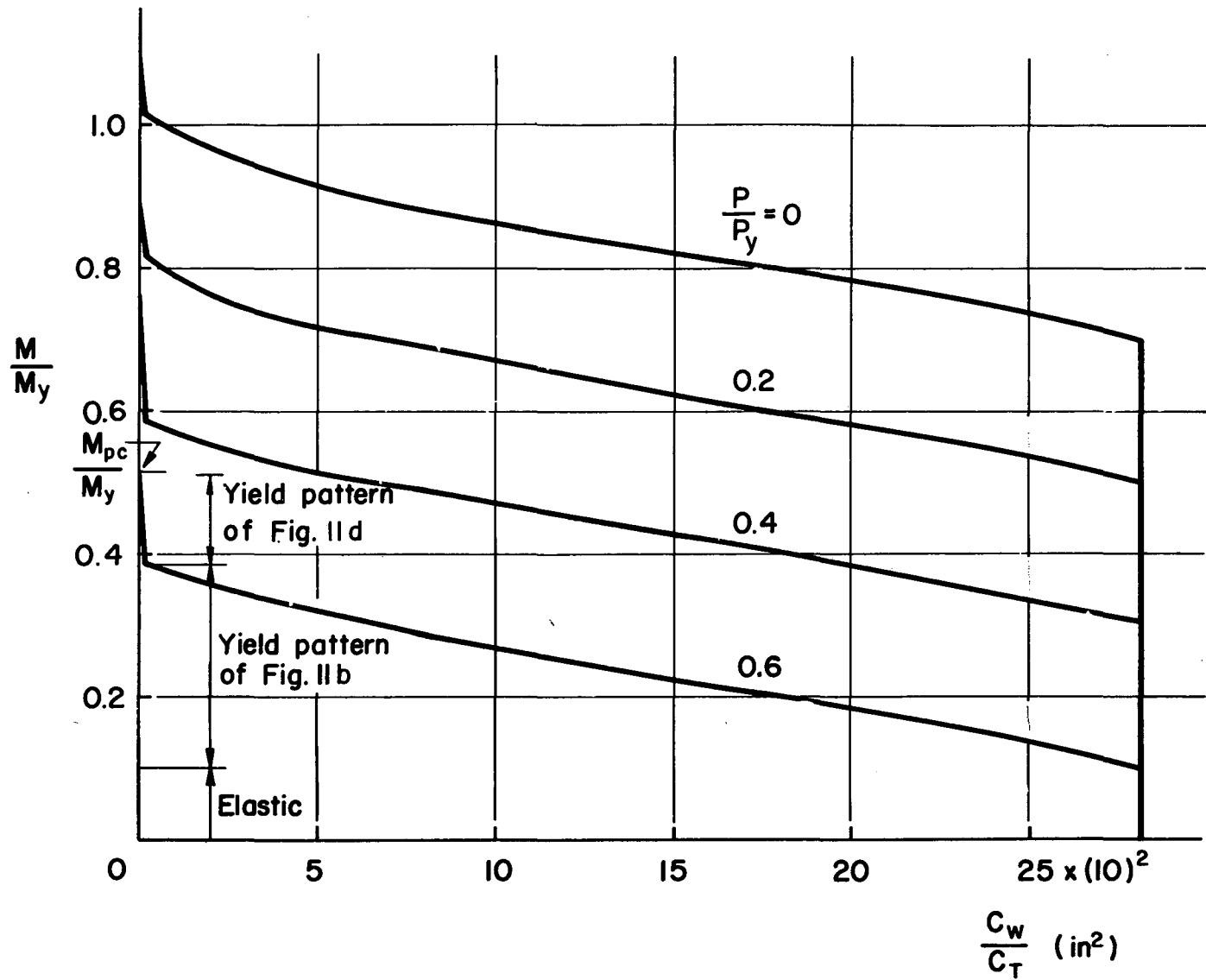


Fig. 14  $M/M_y$  versus  $C_w/C_T$  Curves

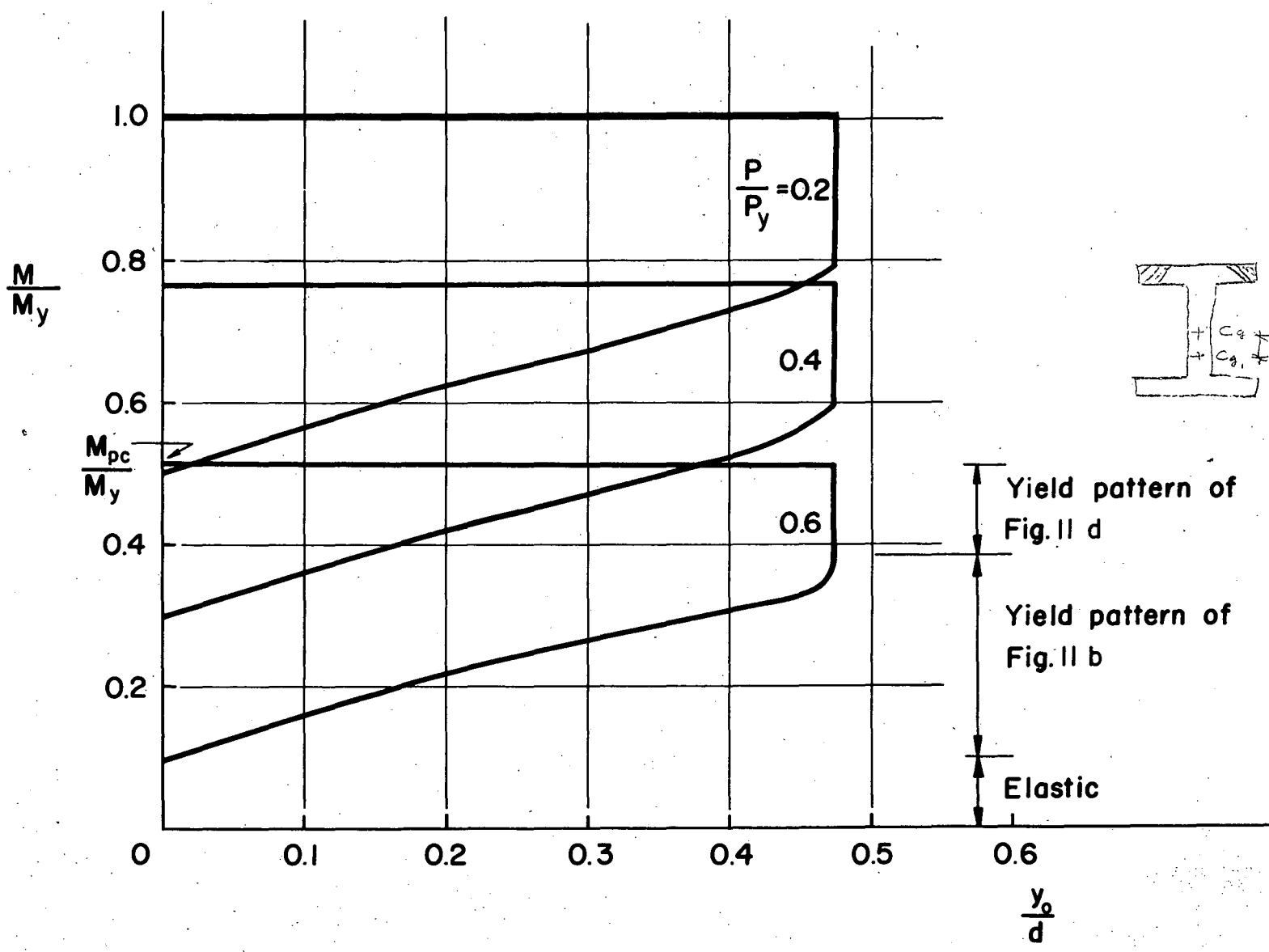


Fig. 15  $M/M_y$  versus  $y_o/d$  Curves

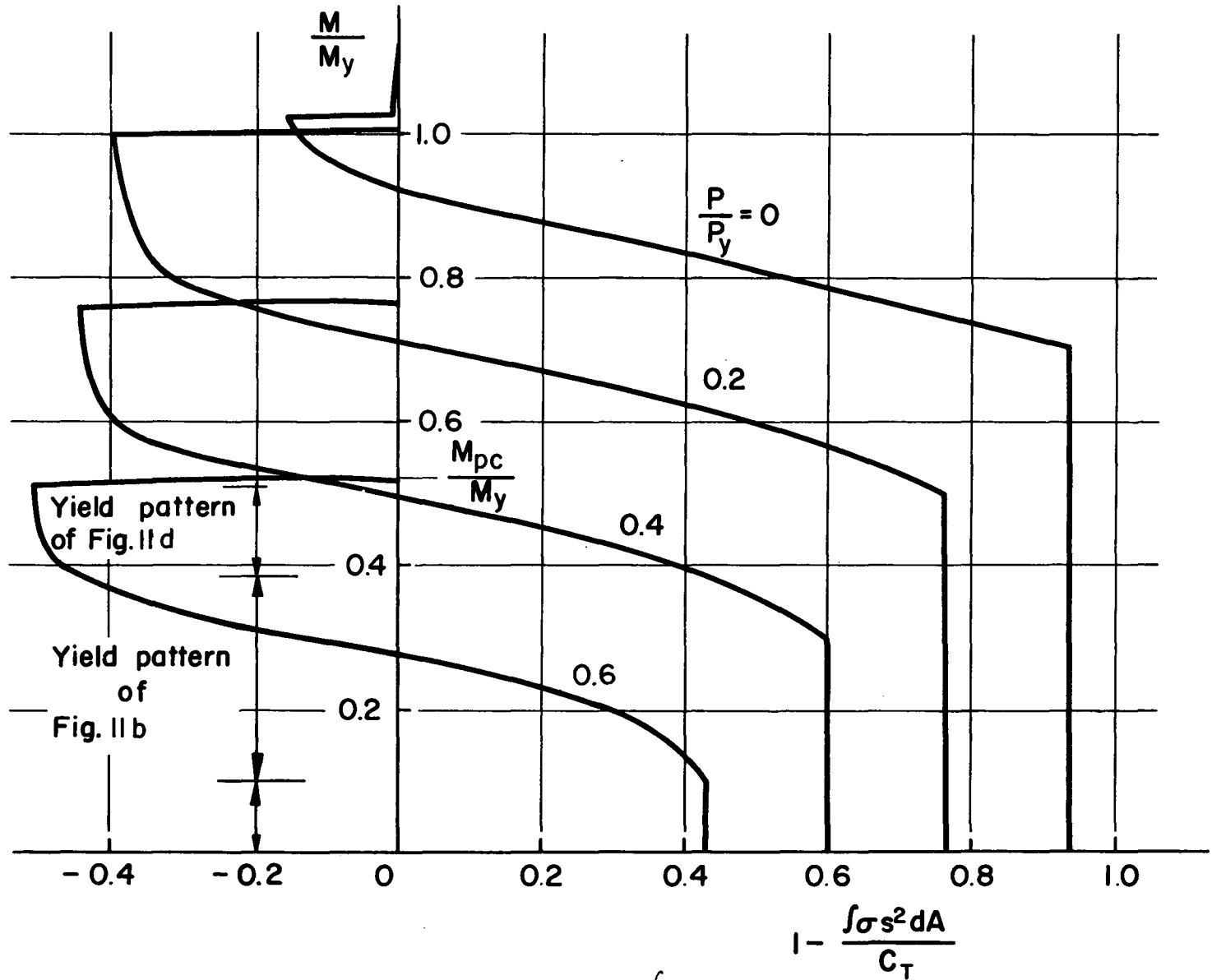


Fig. 16  $M/M_y$  versus  $1 - \frac{\int_A \sigma s^2 dA}{C_T}$  Curves

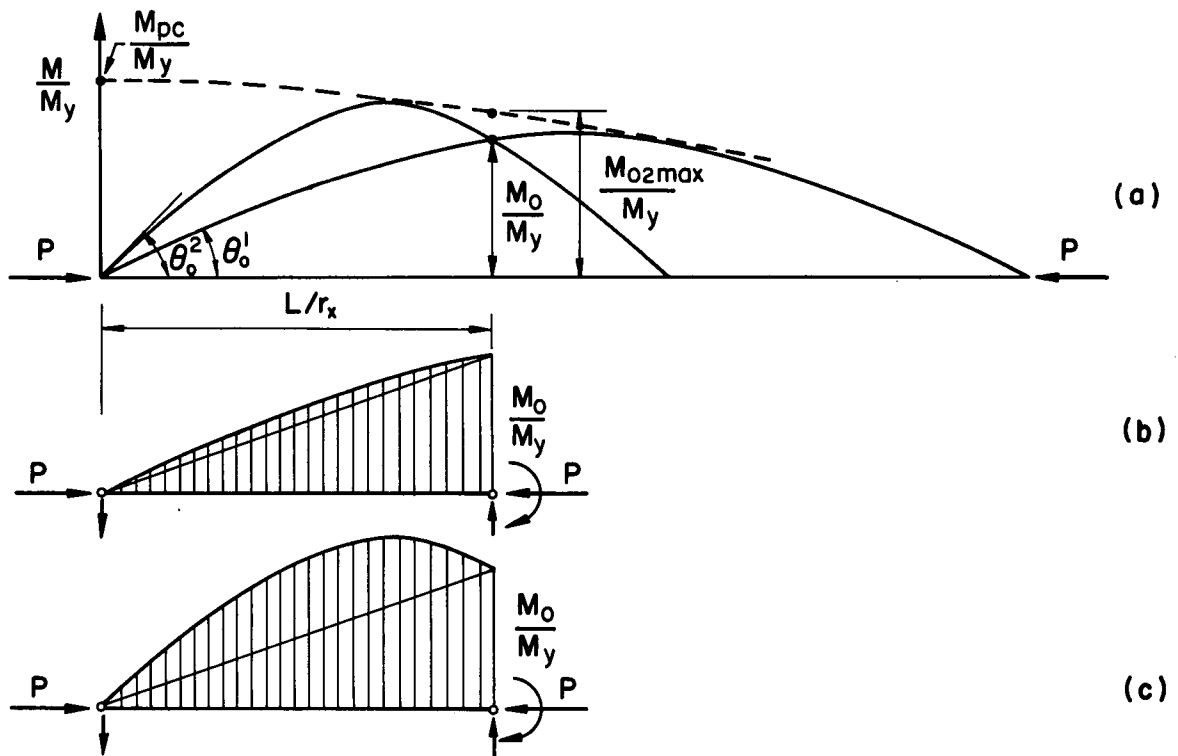


Fig. 17 Column Deflection Curves and Beam-Columns

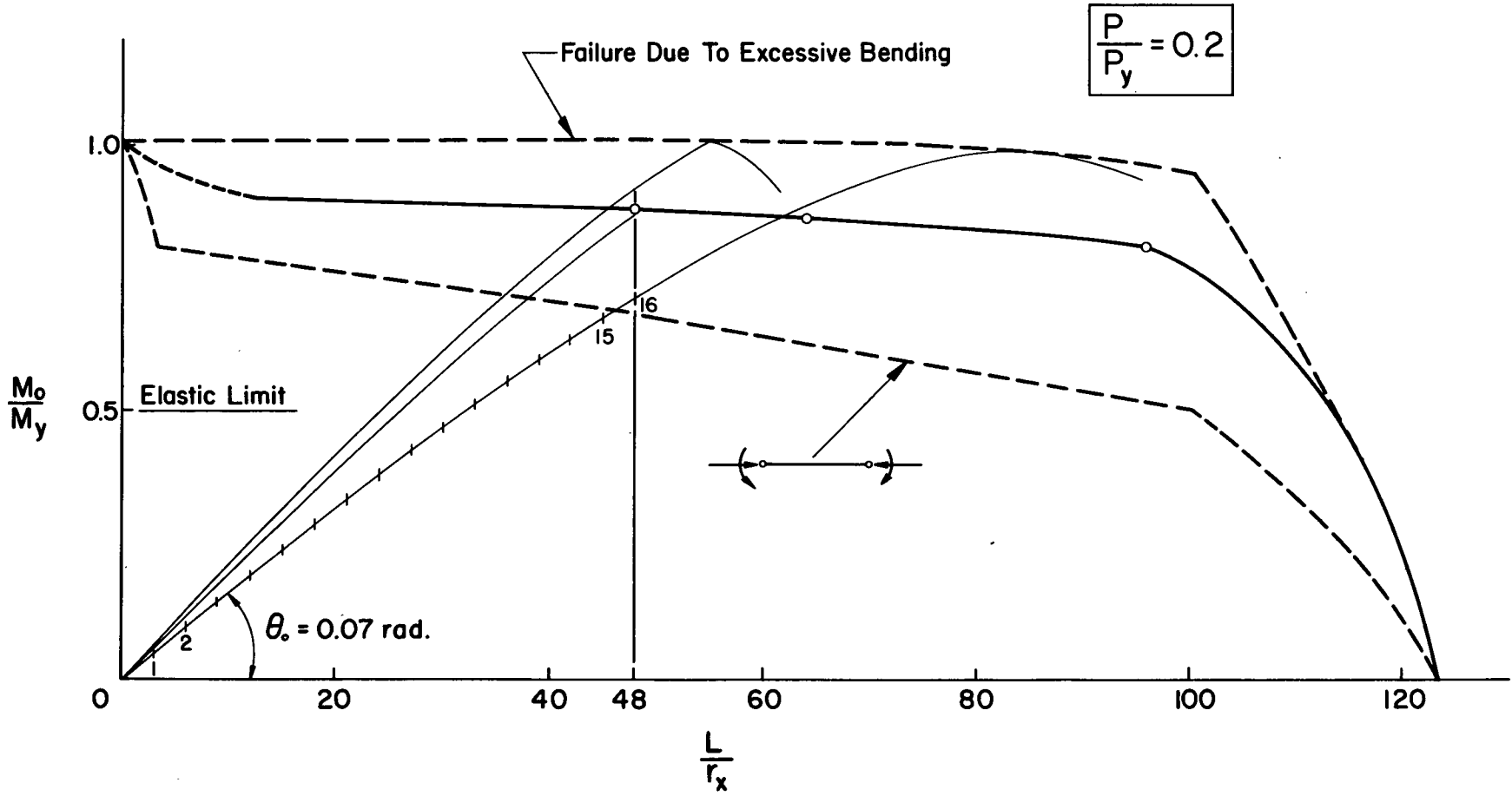


Fig. 18 General Procedures for Solution of the Problem

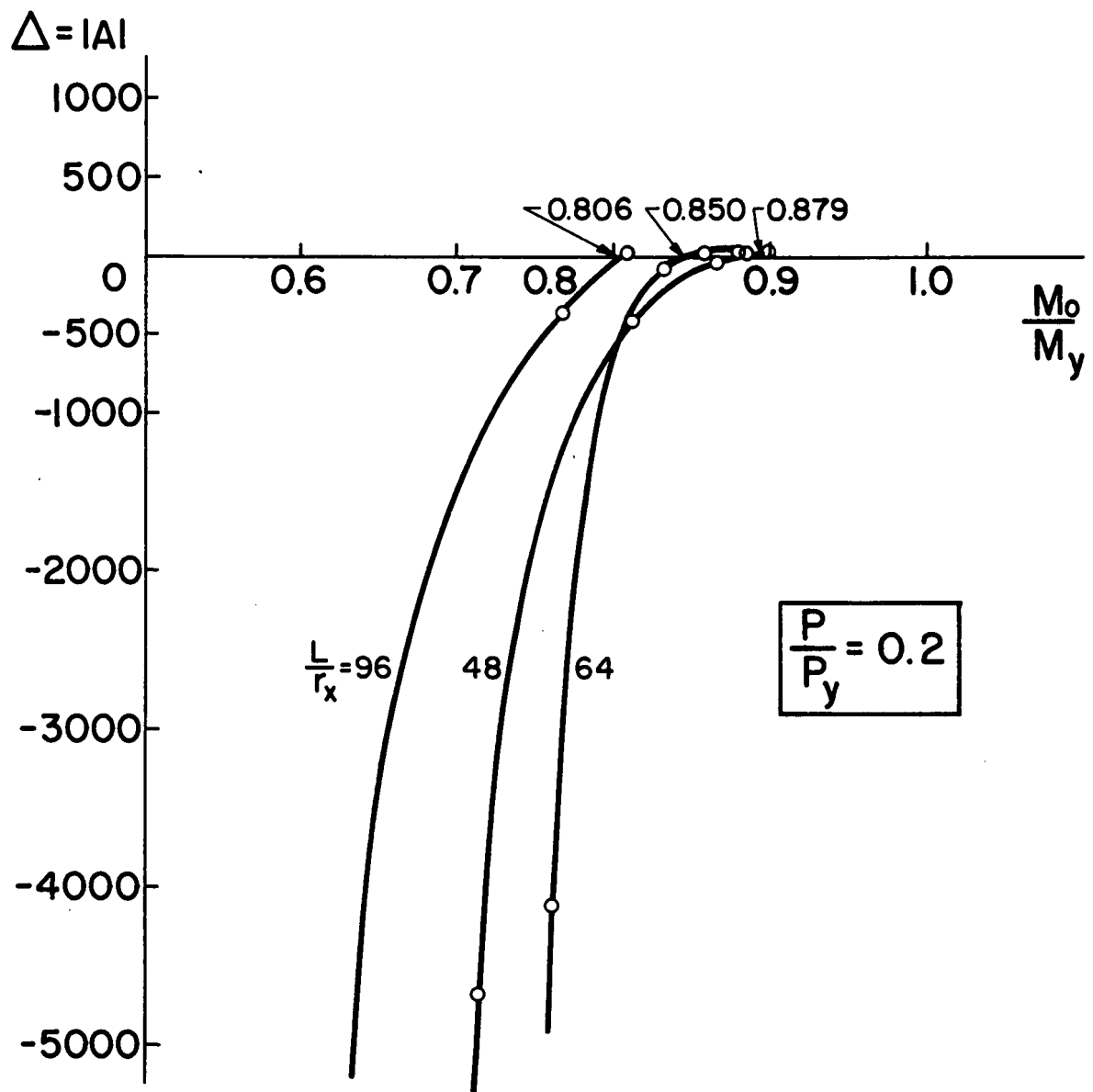


Fig. 19  $|A|$  versus  $M_0/M_y$  Curves for  $P = 0.2P_y$

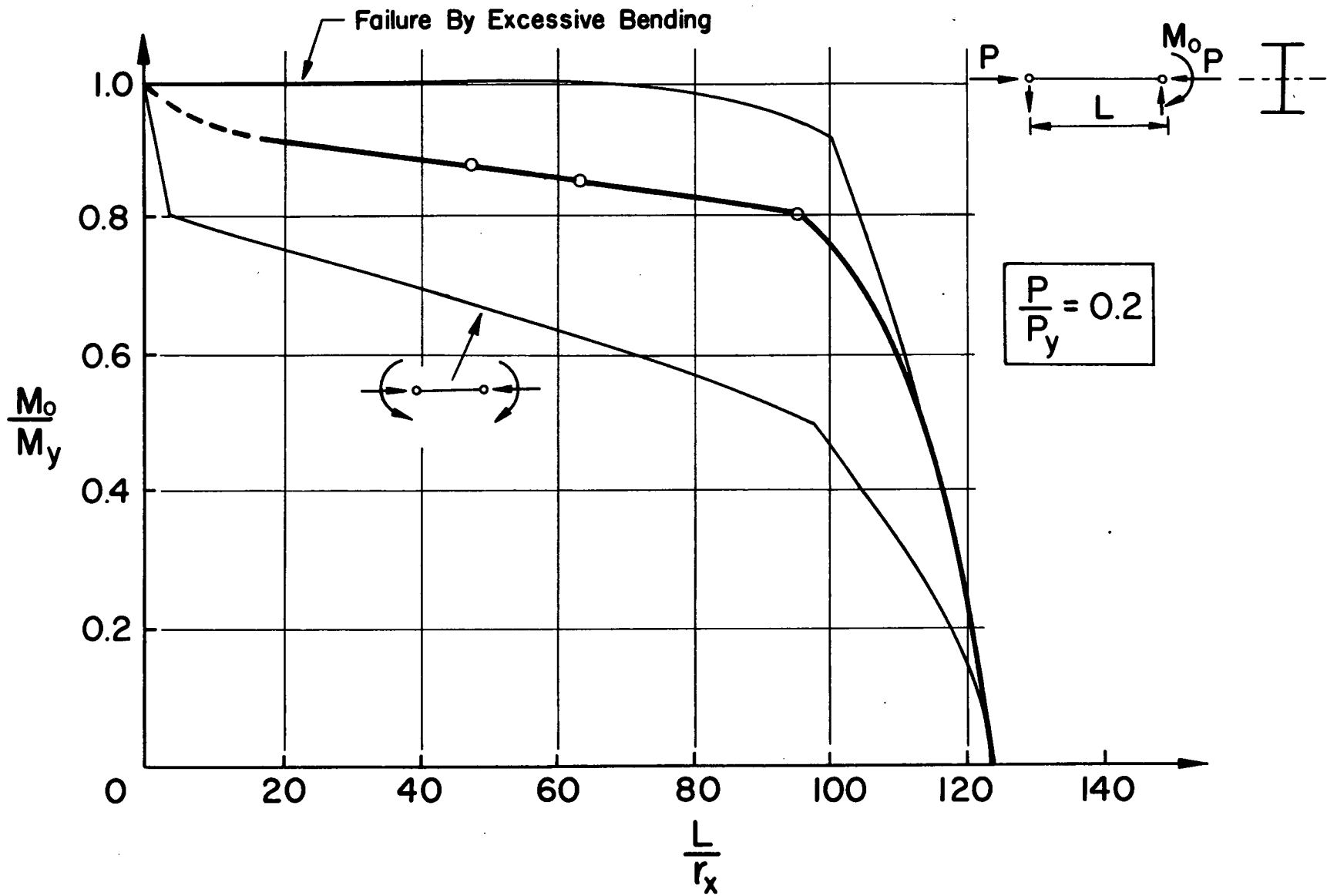


Fig. 20 Lateral-Torsional Buckling Strength Curves for  
 $P/P_y = 0.2$



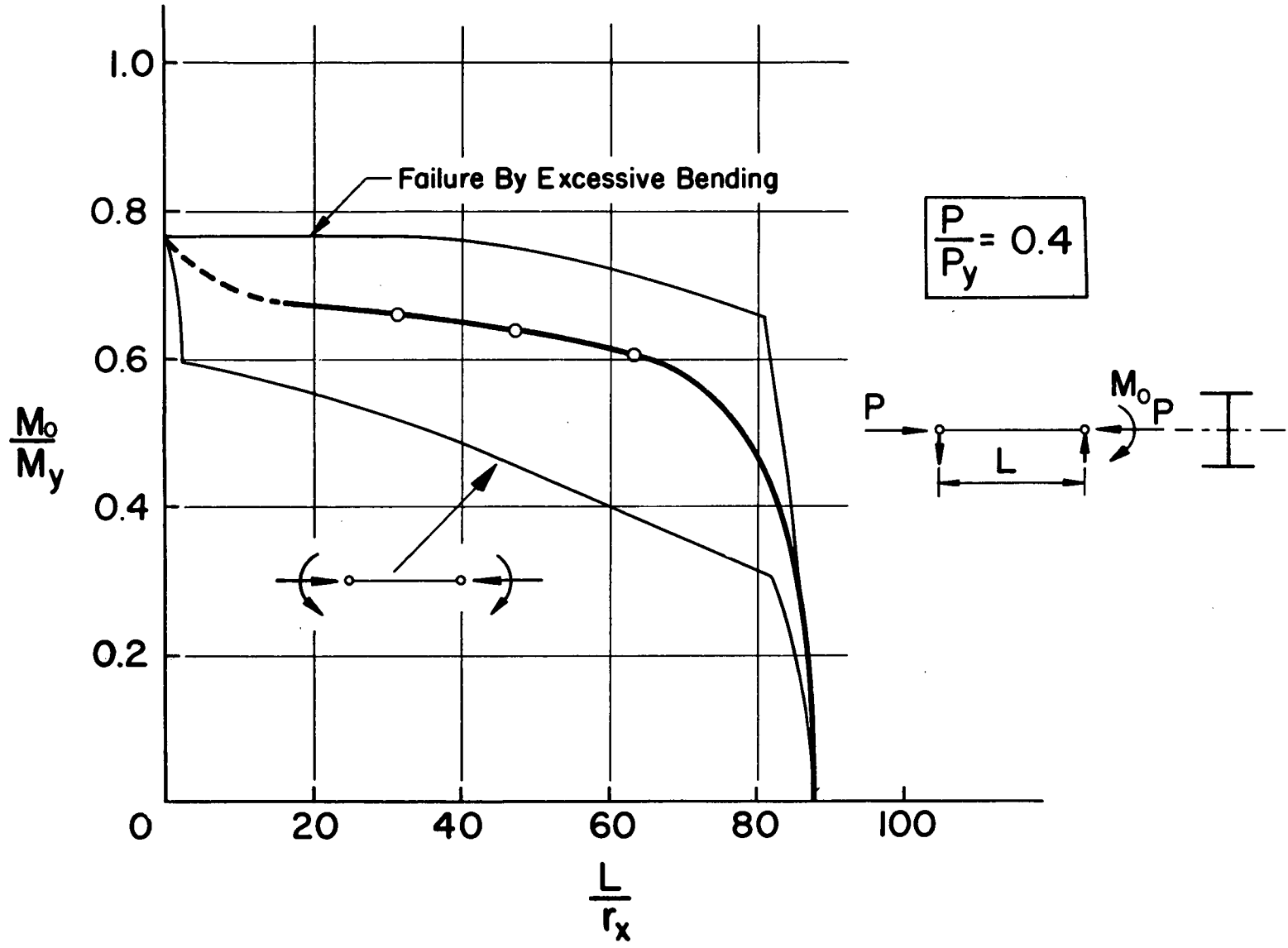


Fig. 21 Lateral-Torsional Buckling Strength Curves  
for  $P/P_y = 0.4$

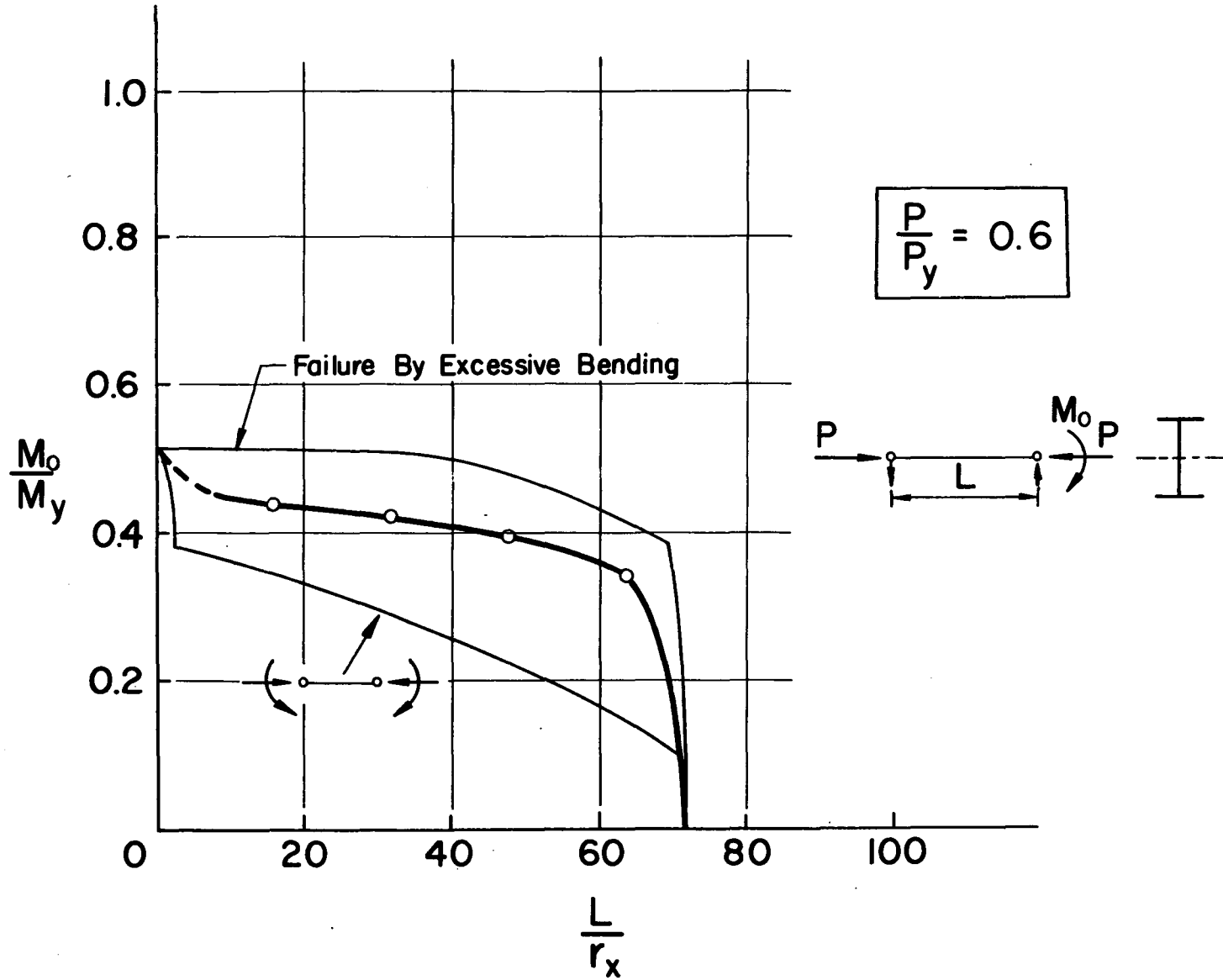


Fig. 22 Lateral-Torsional Buckling Strength Curves  
for  $P/P_y = 0.6$

IX. REFERENCES

1. Bleich, F.  
BUCKLING STRENGTH OF METAL STRUCTURES,  
Chapters 3 and 4, McGraw-Hill, New York,  
1952
2. Timoshenko, S.; Gere, J. M.  
THEORY OF ELASTIC STABILITY,  
Chapters 5 and 6, McGraw-Hill, New York,  
1961
3. Galambos, T. V.; Ketter, R. L.  
COLUMNS UNDER COMBINED BENDING AND THRUST,  
ASCE Trans., Vol. 126, Part I, p.1, 1961
4. Van Kuren, C.; Galambos, T. V.  
BEAM-COLUMN EXPERIMENTS,  
Fritz Engineering Laboratory Report No.  
205A.30, July 1961
5. Galambos, T. V.; Lay, M. G.  
END-MOMENT END-ROTATION CHARACTERISTICS FOR BEAM-  
COLUMNS,  
Fritz Engineering Laboratory Report No.  
205A.35, May 1962
6. Lee, G. C.  
A SURVEY OF LITERATURE ON THE LATERAL  
INSTABILITY OF BEAMS,  
Welding Research Council Bulletin 63,  
p. 50, August 1960
7. Neal, B. G.  
THE LATERAL INSTABILITY OF YIELDED MILD STEEL  
BEAMS OF RECTANGULAR CROSS SECTION,  
Phil., Trans. of Royal Society, Vol. 242,  
Series A, January 1950
8. Wittrick, W. H.  
LATERAL INSTABILITY OF RECTANGULAR BEAMS OF  
STRAIN-HARDENING MATERIAL UNDER UNIFORM BENDING,  
Journal of Aeronautical Science, 19 (12), 835,  
December 1952

9. Horne, M. R.  
CRITICAL LOADING CONDITIONS OF ENGINEERING  
STRUCTURES,  
Ph.D. Dissertation, Cambridge University, 1950
10. White, M. W.  
THE LATERAL-TORSIONAL BUCKLING OF YIELDED  
STRUCTURAL STEEL MEMBERS,  
Ph.D. Dissertation, Lehigh University, 1956
11. Lee, G. C.  
INELASTIC LATERAL INSTABILITY OF BEAMS AND  
THEIR BRACING REQUIREMENTS,  
Ph.D. Dissertation, Lehigh University,  
1960
12. Lee, G. C.; Galambos, T. V.  
POST-BUCKLING STRENGTH OF WIDE-FLANGE BEAMS,  
Proc. of ASCE, Vol. 88, No. EM1, February, 1962
13. Galambos, T. V.  
INELASTIC LATERAL BUCKLING OF BEAMS,  
Fritz Engineering Laboratory Report No. 205A.28,  
Lehigh University, October, 1960
14. Galambos, T. V.  
INELASTIC LATERAL-TORSIONAL BUCKLING OF  
ECCENTRICALLY LOADED WIDE-FLANGE BEAMS  
Ph.D. Dissertation, Lehigh University, 1959
15. Fukumoto, Y.  
INELASTIC LATERAL-TORSIONAL BUCKLING OF BEAM-  
COLUMNS,  
Ph.D. Dissertation, Lehigh University, 1963
16. Ketter, R. L.; Kaminsky, E. L.; Beedle, L. S.  
PLASTIC DEFORMATIONS OF WIDE-FLANGE BEAM-  
COLUMNS,  
ASCE Trans. Vol. 120, p.1058, 1955
17. Reuss, A.  
BERÜCKSICHTIGUNG DER ELASTISCHEN FORMÄNDERUNG IN  
DER PLASTIZITÄTSTHEORIE,  
Z. angew. Math. & Mech., Vol. 10, p.226, 1930

18. Hill, R.; Siebel, M. P. L.  
ON COMBINED BENDING AND TWISTING OF THIN TUBES  
IN THE PLASTIC RANGE,  
Phil. Mag. 42 (7), p.772, 1951
19. Prager, W.; Hodge, P. G.  
THEORY OF PERFECTLY PLASTIC SOLIDS,  
John Wiley & Sons, New York, 1951
20. Ojalvo, M.  
RESTRAINED COLUMNS,  
Ph.D. Dissertation, Lehigh University, 1960
21. Ojalvo, M.; Fukumoto, Y.  
NOMOGRAPHS FOR THE SOLUTION OF BEAM-COLUMN  
PROBLEMS,  
Welding Research Council Bulletin No. 78,  
June, 1962

---

DATE

